Brain Structure and Function (2021) 226:2561–2583
https://doi.org/10.1007/s00429-021-02352-2

ORIGINAL ARTICLE

A quantitative analysis of cerebellar anatomy in birds

Felipe Cunha[1] · Cristian Gutiérrez-Ibáñez[2] · Kelsey Racicot[1] · Douglas R. Wylie[2] · Andrew N. Iwaniuk[1]

Received: 17 May 2021 / Accepted: 26 July 2021 / Published online: 6 August 2021

Abstract

The cerebellum is largely conserved in its circuitry, but varies greatly in size and shape across species. The extent to which differences in cerebellar morphology is driven by changes in neuron numbers, neuron sizes or both, remains largely unknown. To determine how species variation in cerebellum size and shape is reflective of neuron sizes and numbers requires the development of a suitable comparative data set and one that can effectively separate different neuronal populations. Here, we generated the largest comparative dataset to date on neuron numbers, sizes, and volumes of cortical layers and surface area of the cerebellum across 54 bird species. Across different cerebellar sizes, the cortical layers maintained relatively constant proportions to one another and variation in cerebellum size was largely due to neuron numbers rather than neuron sizes. However, the rate at which neuron numbers increased with cerebellum size varied across Purkinje cells, granule cells, and cerebellar nuclei neurons. We also examined the relationship among neuron numbers, cerebellar surface area and cerebellar folding. Our estimate of cerebellar folding, the midsagittal foliation index, was a poor predictor of surface area and number of Purkinje cells, but surface area was the best predictor of Purkinje cell numbers. Overall, this represents the first comprehensive, quantitative analysis of cerebellar anatomy in a comparative context of any vertebrate. The extent to which these relationships occur in other vertebrates requires a similar approach and would determine whether the same scaling principles apply throughout the evolution of the cerebellum.

Keywords Brain allometry · Cerebellum · Neuroanatomy · Brain evolution

Introduction

The anatomy and circuitry of the cerebellum is largely conserved across jawed vertebrates (Voogd and Glickstein 1998), but cerebellar size and shape vary considerably across clades (Larsell 1967; Yopak et al. 2017). For example, while non-avian reptiles and amphibians have relatively small cerebella with few folds (i.e., low degree of foliation), mammals and birds have relatively large cerebella that are highly folded (Yopak et al. 2017). Even within vertebrate classes, such as birds, cerebellar morphology varies greatly across species (Iwaniuk et al. 2006, 2007; Sultan and Glickstein 2007). Some of this variation is thought to reflect differences in neuron number and/or neuron size (Herculano-Houzel et al. 2014), and thus neural processing related to, for example, cognitive processing (Hall et al. 2013; Iwaniuk et al. 2009; Smaers et al. 2018) and locomotion (Iwaniuk et al. 2007; Larsell 1967). However, the extent to which interspecific variation in cerebellum size and morphology arises from neuron sizes and numbers remains uncertain. Recent studies on total neuron numbers in the cerebellum indicate that the allometric relationship between the number of neurons and cerebellar mass is largely conserved across species (Herculano-Houzel et al. 2015a; Jardim-Messeder et al. 2017; Olkowicz et al. 2016), with only a couple of clades deviating from this general "scaling rule" (Herculano-Houzel et al. 2014, 2015a).

Of the mammal species studied thus far, two clades diverge from a general allometric relationship between cerebellar mass and total number of neurons such that they have higher neuronal densities in the cerebellum: primates and eulipotyphlans (shrews, moles, and hedgehogs) (Herculano-Houzel et al. 2014, 2015a). This increased neuronal density accompanies a highly folded cerebellum and an expansion

✉ Felipe Cunha
felipebrcunha@gmail.com

[1] Department of Neuroscience, University of Lethbridge, 4401 University Dr. W, Science & Academic Building, SA8150, Lethbridge, AB T1K 6T5, Canada

[2] Department of Biological Sciences, University of Alberta, Edmonton, AB, Canada

of the cerebellar hemispheres in primates (MacLeod et al. 2003; Smaers et al. 2018), but no comparable changes in eulipotyphlan cerebella. In birds, songbirds and parrots also have higher neuronal densities in the cerebellum compared with other avian clades (Olkowicz et al. 2016), but both songbirds and parrots also tend to have relatively smaller and more foliated cerebella (Iwaniuk et al. 2005, 2006). Thus, an increase in neuronal density in the cerebellum is associated with larger or smaller cerebella, a more folded cerebellar cortex or no discernible gross anatomical changes at all. These mixed results across mammals and birds means that the relationship between neuron numbers and cerebellar size and shape remains unclear.

All of the neuron-volume scaling relationships described above were obtained through the use of the isotropic fractionator (Herculano-Houzel and Lent 2005), which provides accurate estimates of total neuron numbers in dissectible brain regions (Herculano-Houzel et al. 2015c; Ngwenya et al. 2017), but does not yet allow for the separation of different neuronal populations within the cerebellum. Further, the isotropic fractionator method does not include Purkinje cells because they do not express NeuN (Apps and Hawkes 2009; Mullen et al. 1992). Like any larger brain region, the cerebellum is comprised of different types of neurons connected to each other in different ways (Yopak et al. 2017). For example, while granule cells receive input from mossy fibers and project to Purkinje cells through parallel fibers, Purkinje cells also receive input from climbing fibers and are the sole source of output to the cerebellar and vestibular nuclei (Apps and Hawkes 2009). The numbers of these different neuronal populations could vary at a different rate relative to total cerebellar size. Determining whether different neuronal populations increase with cerebellum size at different rates would provide novel and more specific insights into the functional consequences of a relatively larger and/or more folded cerebellum. For example, if some clades or cerebellar morphologies have more Purkinje cells, this could indicate enhanced output processing from the cerebellar cortex.

Another caveat of the isotropic fractionator method is that neuron size is not measured directly, but rather is inferred as inversely proportional to neuronal density (Herculano-Houzel et al. 2014). This is because the method relies on rupturing cell membranes to stain nuclei. Scaling of neuron size with cerebellum size, or for that matter most brain regions, across species, therefore, remains largely unexplored (but see Stevens 1969; Teeter and Stevens 2011). Just as different neuronal populations might vary in neuron number–region volume relationships, the scaling of cell size could also vary among different types of neurons. This is especially true for the cerebellum, which contains both the largest neurons (Purkinje cells) and the smallest neurons (granule cells) in the brain (Lange 1982). In fact, across galliform birds (e.g., quail, partridge, pheasant), Purkinje cell size is positively correlated with the size of the cerebellum, while granule cell size is not (Cunha et al. 2020). Thus, instead of inferring the average size of total cerebellar neurons from neuronal density (Herculano-Houzel et al. 2014), actual measurements of neuron size are needed to determine to what extent species differences in cerebellum size are driven by neuron numbers and/or sizes.

As noted above, the cerebellum not only varies in overall size, but also morphology. More specifically, the degree of folding, referred to as foliation, varies greatly across and within clades (Cunha et al. 2020; Iwaniuk et al. 2006; Yopak et al. 2007). Such variation is thought to reflect behavioural differences across species. For example, fast-swimming sharks performing complex manoeuvres tend to have a more foliated cerebellum than slow-moving sharks (Yopak et al. 2007) and birds that build more complex nests (Hall et al. 2013) or use tools (Iwaniuk et al. 2009) have relatively more folded cerebella than other species. An assumption that underlies these studies is that a higher degree of foliation reflects an increase in the surface area of the cerebellum relative to cerebellar volume, therefore, allowing more cells within a given volume and an increase in processing capacity (Hall et al. 2013; Iwaniuk et al. 2009). Within galliform birds, the degree of foliation is positively correlated with the number of cerebellar neurons, but neuronal populations differ in their allometric relationships with the degree of foliation (Cunha et al. 2020). Whether these same patterns can be generalized across other clades remains to be determined, but is critical to understand the functional implications of cerebellar foliation. For example, if a more foliated cerebellum has more Purkinje cells, which would reflect greater output from the cerebellar cortex to the cerebellar and vestibular nuclei. Thus, a detailed investigation on the cellular scaling of the cerebellum, combined with what is known of cerebellar circuitry, would provide novel insights into the functional consequences of species differences in not only cerebellar size, but also morphology.

To address these key issues in cerebellar evolution, we provide the most detailed quantitative analysis of cerebellar anatomy conducted in a comparative context so far. We quantified the volumes of different layers of the cerebellar cortex, surface area of the Purkinje cell layer, cerebellar foliation and the sizes and numbers of Purkinje cells, granule cells, and cerebellar nuclei neurons across 54 avian species. Using this data set, we calculated allometric relationships among all variables to test whether: (i) cerebellar layers increase in volume at a same rate across species; (ii) different neuronal populations scale with cerebellar size at the same rate; (iii) a higher degree of cerebellar foliation is associated with an increase in the surface area of the Purkinje cell layer and thus number of cerebellar neurons

(e.g., Purkinje cells); and (iv) if there are quantitative differences in the cerebellar anatomy among clades.

Methods

Specimens

We obtained measurements of the cerebella from 54 species representing 18 orders of birds (Fig. 1; Tables 1, 2, 3). With the exception of some galliform species (*Bonasa umbellus, Coturnix japonica,* and *Perdix perdix*; Cunha et al. 2020), a single individual was sampled per species. As described elsewhere, our brain collection is derived from specimens obtained from wildlife sanctuaries, veterinary clinics in Australia and hunters in Canada and New Zealand (Corfield et al. 2013, 2015) and the methods of collection of the specimens adhered to the guidelines of the Canada Council for Animal Care. The heads of these specimens were immersion fixed in 4% buffered paraformaldehyde for at least 2 weeks. The brains were extracted, weighed, and stored in paraformaldehyde. The brains then were place in 30% sucrose in 0.1 M phosphate buffer until they sank (for cryoprotection), embedded in gelatin, sectioned on a freezing stage microtome in the sagittal plane at a thickness of 40 µm and every section collected in 0.1 M phosphate buffered saline.

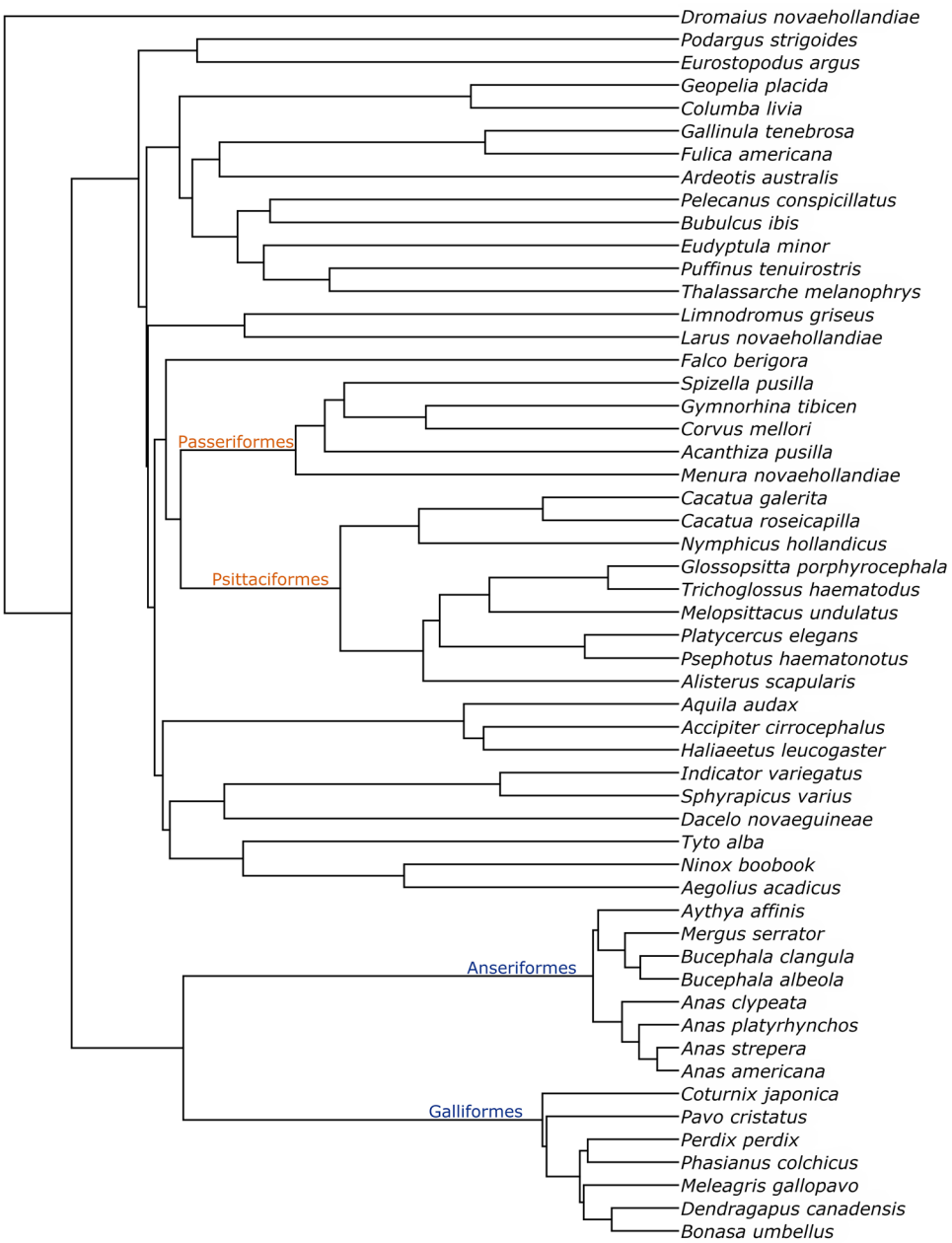

Fig. 1 Phylogeny of the species analyzed in this study. The orders Passeriformes (songbirds), Psittaciformes (parrots), Anseriformes (waterfowls), and Galliformes (chicken-like birds) are indicated on the branches

Table 1 A list of the avian species analyzed and their respective brain volumes, cerebellum volumes, molecular layer volumes, granule cell layer volumes, white matter volumes, surface area of the Purkinje cell layer, and cerebellar foliation index (CFI)

Order	Common name/species	Brain Volume (mm^3)	Cerebellum Volume (mm^3)	Molecular layer Volume (mm^3)	Granule cell layer Volume (mm^3)	White matter Volume (mm^3)	Purkinje cell layer, surface area (μm^2)	Cerebellar foliation index
Accipitriformes	Collared sparrowhawk (*Accipiter cirrocephalus*)	4875.483	749.476	331.006	224.770	181.966	1,054,295,727	4.40
	Wedge-tailed eagle (*Aquila audax*)	15,997.104	1466.816	685.260	406.260	367.796	1,557,879,727	4.68
	White-bellied sea eagle (*Haliaeetus leucogaster)*	12,540.540	1108.880	507.160	289.580	312.360	964,970,443	4.57
Anseriformes	American wigeon (*Anas americana)*	5245.173	549.587	271.366	157.114	104.845	756,665,832	3.72
	Northern shoveler (*Anas clypeata*)	3288.513	279.091	133.606	88.934	56.550	378,222,471	3.14
	Mallard (*Anas platyrhynchos*)	6216.255	560.058	286.351	151.064	109.660	910,208,725	3.45
	Gadwall (*Anas strepera*)	4324.324	510.189	223.622	154.310	120.928	684,181,960	3.37
	Lesser scaup (*Aythya affinis*)	4546.139	437.920	213.370	132.678	79.014	637,152,788	3.76
	Bufflehead (*Bucephala albeola)*	4440.154	559.080	271.490	173.534	102.730	621,147,084	3.60
	Common goldeneye (*Bucephala clangula*)	5961.390	685.382	356.603	203.059	125.518	942,512,966	4.11
	Red-breasted merganser (*Mergus serrator*)	4247.104	442.431	178.120	148.054	111.274	614,832,009	3.56
Caprimulgiformes	Spotted nightjar (*Eurostopodus argus*)	1012.548	137.935	61.280	43.535	30.265	212,361,215	3.01
	Tawny frogmouth (*Podargus strigoides*)	5943.050	442.086	226.194	134.145	69.455	460,317,436	3.35
Casuariiformes	Emu (*Dromaius novaehollandiae*)	27,750	3352.930	1576.430	944.610	766.880	2,966,617,590	4.94
Charadriiformes	Silver gull (*Larus novaehollandiae*)	2941.120	325.830	168.384	92.404	65.768	404,151,167	4.02
	Short-billed dowitcher (*Limnodromus griseus*)	1338.031	102.960	51.696	31.601	18.101	176,856,625	3.38

Table 1 (continued)

Order	Common name/ species	Brain Volume (mm^3)	Cerebellum Volume (mm^3)	Molecular layer Volume (mm^3)	Granule cell layer Volume (mm^3)	White matter Volume (mm^3)	Purkinje cell layer, surface area (μm^2)	Cerebellar foliation index
Columbiformes	Rock dove (*Columba livia*)	2343.436	296.410	135.962	91.635	63.283	500,813,356	4.16
	Peaceful dove (*Geopelia placida*)	776.062	85.2732	40.034	28.0512	14.767	153,994,538	2.97
Coraciiformes	Laughing kookaburra (*Dacelo novaeguineae*)	3970.077	389.618	174.675	135.877	78.870	551,543,759	3.55
Falconiformes	Brown falcon (*Falco berigora*)	6031.853	638.496	323.704	189.022	115.819	680,062,357	3.87
Galliformes	Ruffed grouse (*Bonasa umbellus*)	2288.120	324.170	139.995	84.374	55.716	497,138,294	4.01
	Japanese quail (*Coturnix japonica*)	936.390	118.867	57.609	33.693	17.387	208,022,535	3.53
	Spruce grouse (*Dendragapus canadensis*)	1944.500	340.710	157.025	88.557	57.332	498,244,020	3.75
	Turkey (*Meleagris gallopavo*)	5905.975	945.435	408.138	248.492	186.467	1,309,051,327	5.29
	Indian peafowl (*Pavo cristatus*)	6070.785	749.080	329.097	187.214	129.592	947,227,067	4.29
	Grey partridge (*Perdix perdix*)	2027.027	182.530	88.141	51.173	30.472	325,485,310	3.73
	Ring-necked pheasant (*Phasianus colchicus*)	4060.039	397.133	184.581	101.074	71.064	541,238,255	4.01
Gruiformes	American coot (*Fulica americana*)	2718.919	242.208	119.614	74.498	42.710	390,131,670	3.43
	Dusky moorhen (*Gallinula tenebrosa*)	2726.544	308.984	152.184	87.475	69.678	371,087,600	3.21
Otidiformes	Australian bustard (*Ardeotis australis*)	10,500.965	1257.190	592.004	349.836	304.556	1,351,531,180	4.69

Table 1 (continued)

Order	Common name/ species	Brain Volume (mm^3)	Cerebellum Volume (mm^3)	Molecular layer Volume (mm^3)	Granule cell layer Volume (mm^3)	White matter Volume (mm^3)	Purkinje cell layer, surface area (μm^2)	Cerebellar foliation index
Passeriformes	Brown thornbill (*Acanthiza pusilla*)	434.363	37.080	18.536	12.103	5.632	105,390,527	3.45
	Little raven (*Corvus mellori*)	9833.977	689.292	371.034	177.280	134.669	1,065,446,231	5.34
	Australian magpie (*Gymnorhina tibicen*)	5665.058	412.762	205.552	114.084	86.645	797,050,699	4.92
	Superb lyrebird (*Menura novaehollandiae*)	10,163.127	819.282	405.340	240.878	163.150	931,334,099	4.29
	Field sparrow (*Spizella pusilla*)	579.150	46.866	19.112	18.035	9.691	114,769,622	3.49
Pelecaniformes	Cattle egret (*Bubulcus ibis*)	4025.096	383.994	194.863	113.376	70.776	513,045,821	4.26
	Australian pelican (*Pelecanus conspicillatus*)	22,500	2173.060	1117.048	584.068	468.124	2,297,435,251	4.89
Piciformes	Scaly-throated honeyguide (*Indicator variegatus*)	800	109.910	57.620	37.125	12.780	216,155,679	3.57
	Yellow-bellied sapsucker (*Sphyrapicus varius*)	1442.761	125.878	49.392	46.447	27.032	294,672,035	3.81
Procellariiformes	Short-tailed shearwater (*Puffinus tenuirostris*)	4757.722	756.520	394.480	231.700	116.220	1,103,366,504	4.25
	Black-browed albatross (*Thalassarche melanophris*)	14,129.344	2047.780	1020.916	574.374	424.960	2,811,851,152	5.51

Table 1 (continued)

Order	Common name/ species	Brain Volume (mm^3)	Cerebellum Volume (mm^3)	Molecular layer Volume (mm^3)	Granule cell layer Volume (mm^3)	White matter Volume (mm^3)	Purkinje cell layer, surface area (μm^2)	Cerebellar foliation index
Psittaciformes	Australian king parrot (*Alisterus scapularis*)	4901.544	322.714	157.542	92.083	67.942	517,671,690	4.41
	Sulphur-crested cockatoo (*Cacatua galerita*)	13,937.259	1048.852	501.600	297.350	222.378	1,453,018,054	5.56
	Galah (*Cacatua roseicapilla*)	7455.598	479.634	226.720	141.215	104.328	643,265,073	4.80
	Purple-crowned lorikeet (*Glossopsitta porphyrocephala*)	1855.212	137.923	62.165	43.819	31.334	235,961,485	3.78
	Budgerigar (*Melopsittacus undulatus*)	1486.486	156.575	68.840	40.730	42.585	283,101,554	3.90
	Cockatiel (*Nymphicus hollandicus*)	2161.197	220.004	105.120	60.530	49.687	381,440,513	4.17
	Crimson rosella (*Platycercus elegans*)	3628.378	225.094	100.210	69.516	50.213	369,803,274	4.14
	Red-rumped parrot (*Psephotus haematonotus*)	1798.262	135.238	62.086	41.098	29.066	277,353,038	3.79
	Rainbow lorikeet (*Trichoglossus haematodus*)	3333.977	190.924	97.187	54.919	35.133	395,266,155	4.30
Sphenisciformes	Little penguin (*Eudyptula minor*)	7583.977	1365.146	777.134	340.858	225.882	1,561,508,578	4.91
Strigiformes	Northern sawwhet owl (*Aegolius acadicus*)	2857.143	239.494	95.868	80.798	54.648	380,425,115	3.70
	Australian boobook (*Ninox boobook*)	6338.803	377.972	174.938	122.534	69.491	452,608,686	3.61
	Barn owl (*Tyto alba*)	7142.857	397.556	186.926	122.954	77.710	559,195,713	3.79

For some specimens, the cerebella were first dissected from the brain by cutting through the cerebellar peduncles and processed in the same way as the intact brains. For all species, every other section (1:2 series) was mounted onto gelatinized slides, stained with thionin acetate, dehydrated through a graded ethanol series, cleared in Hemo-De (Thermo Fisher Scientific, #HD-150) and coverslipped with Permount (Thermo Fisher Scientific, #SP15-150).

Table 2 Numbers (#) of Purkinje cells, granule cells, and cerebellar nuclei neurons across species analyzed

Order	Common name/species	#Purkinje cells	#Granule cells	#Cerebellar nuclei neurons
Accipitriformes	Collared sparrowhawk (*Accipiter cirrocephalus)*	897,955	890,894,656	169,550
	Wedge-tailed eagle (*Aquila audax*)	1,267,441	1,149,562,112	242,359
	White-bellied sea eagle (*Haliaeetus leucogaster)*	1,005,487	923,455,360	172,132
Anseriformes	American wigeon (*Anas americana*)	624,585	442,898,400	116,930
	Northern shoveler (*Anas clypeata*)	457,616	285,671,744	114,034
	Mallard (*Anas platyrhynchos*)	907,034	635,422,912	112,362
	Gadwall (*Anas strepera*)	617,042	480,030,240	137,483
	Lesser scaup (*Aythya affinis*)	581,555	447,906,304	148,472
	Bufflehead (*Bucephala albeola)*	511,940	442,348,640	88,386
	Common goldeneye (*Bucephala clangula*)	1,383,070	606,733,632	145,463
	Red-breasted merganser (*Mergus serrator*)	593,958	457,814,016	98,760
Caprimulgiformes	Spotted nightjar (*Eurostopodus argus*)	169,574	150,813,568	44,861
	Tawny frogmouth (*Podargus strigoides*)	455,900	376,710,656	77,081
Casuariiformes	Emu (*Dromaius novaehollandiae*)	4,735,835	2,584,285,440	357,850
Charadriiformes	Silver gull (*Larus novaehollandiae*)	333,034	302,858,368	70,523
	Short-billed dowitcher (*Limnodromus griseus*)	167,844	78,940,320	57,750
Columbiformes	Rock dove (*Columba livia*)	523,856	346,092,704	81,118
	Peaceful dove (*Geopelia placida*)	175,798	91,912,584	45,343
Coraciiformes	Laughing kookaburra (*Dacelo novaeguineae*)	543,676	940,231,232	81,467
Falconiformes	Brown falcon (*Falco berigora*)	740,853	652,221,632	80,901
Galliformes	Ruffed grouse (*Bonasa umbellus*)	568,783	307,992,725	105,378
	Japanese quail (*Coturnix japonica*)	402,471	106,524,944	69,634
	Spruce grouse (*Dendragapus canadensis*)	577,257	222,194,016	78,799
	Turkey (*Meleagris gallopavo*)	1,261,079	896,211,904	190,878
	Indian peafowl (*Pavo cristatus*)	904,452	393,968,960	144,161
	Grey partridge (*Perdix perdix*)	451,406	120,762,048	73,693
	Ring-necked pheasant (*Phasianus colchicus*)	586,874	401,393,760	87,841
Gruiformes	American coot (*Fulica americana*)	379,303	319,894,080	76,381
	Dusky moorhen (*Gallinula tenebrosa*)	379,368	258,506,304	96,273
Otidiformes	Australian bustard (*Ardeotis australis*)	954,555	916,399,552	161,511

Table 2 (continued)

Order	Common name/species	#Purkinje cells	#Granule cells	#Cerebellar nuclei neurons
Passeriformes	Brown thornbill (*Acanthiza pusilla*)	172,757	85,635,896	35,690
	Little raven (*Corvus mellori*)	892,424	780,922,368	120,485
	Australian magpie (*Gymnorhina tibicen*)	768,936	814,053,056	93,900
	Superb lyrebird (*Menura novaehollandiae*)	870,097	904,763,584	147,375
	Field sparrow (*Spizella pusilla*)	134,504	75,443,432	30,442
Pelecaniformes	Cattle egret (*Bubulcus ibis*)	429,449	349,358,112	93,184
	Australian pelican (*Pelecanus conspicillatus*)	1,588,855	1,291,263,872	264,139
Piciformes	Scaly-throated honeyguide (*Indicator variegatus*)	210,990	101,545,400	48,422
	Yellow-bellied sapsucker (*Sphyrapicus varius*)	305,975	180,678,592	63,559
Procellariiformes	Short-tailed shearwater (*Puffinus tenuirostris*)	770,170	908,588,288	99,623
	Black-browed albatross (*Thalassarche melanophris*)	2,300,728	1,621,144,960	291,537
Psittaciformes	Australian king parrot (*Alisterus scapularis*)	509,073	348,362,976	88,750
	Sulphur-crested cockatoo (*Cacatua galerita*)	1,254,155	1,022,579,776	168,471
	Galah (*Cacatua roseicapilla*)	617,875	574,456,000	100,342
	Purple-crowned lorikeet (*Glossopsitta porphyrocephala*)	241,327	175,971,680	61,182
	Budgerigar (*Melopsittacus undulatus*)	289,087	155,686,048	59,123
	Cockatiel (*Nymphicus hollandicus*)	376,777	240,051,504	85,989
	Crimson rosella (*Platycercus elegans*)	259,291	271,755,136	82,464
	Red-rumped parrot (*Psephotus haematonotus*)	268,572	180,058,576	48,783
	Rainbow lorikeet (*Trichoglossus haematodus*)	323,122	217,400,720	66,609
Sphenisciformes	Little penguin (*Eudyptula minor*)	1,242,661	970,026,304	155,915
Strigiformes	Northern saw-whet owl (*Aegolius acadicus*)	380,817	265,476,624	53,250
	Australian boobook (*Ninox boobook*)	609,521	436,894,720	139,601
	Barn owl (*Tyto alba*)	451,163	472,394,048	95,436

Volumetric measurements

We measured the volumes of molecular cell layer (ml), granule cell layer (gl), white matter layer including the cerebellar nuclei (wm + cn) and total cerebellum volume (cb) using the Cavalieri method, as implemented in Stereo Investigator software (Microbrightfield Inc., VT, USA), with a 2.5 × objective (n.a. = 0.075) on a Zeiss Axio Imager 2 microscope. The Cavalieri method consists of counting grid points that are inside a region of interest (e.g., molecular layer). Each point has a specific area, and the sum of those areas can be multiplied by the thickness of the tissue and sampling interval (i.e., inverse of the proportion of sections analyzed) to accurately estimate the volume of the entire region (Gundersen et al. 1999; Table S1). Each of the cerebellar layers measured are easily distinguishable from one another (Fig. 2), but the cerebellar nuclei were included with the white matter volume because of the indistinct borders of the cerebellar nuclei in sagittal sections. We, therefore, refer to this as the white matter plus cerebellar nuclei (wm + cn). The Purkinje cell layer is typically a thick, mono-cell layer with some discontinuous gaps between cells in sagittal sections. Hence, calculating the volume of this layer could lead to significant measurement errors. As an alternative, we measured the surface area of Purkinje cell layer, and size and number of Purkinje cells (see below) rather than the volume of the layer. Estimated volumes of all regions of interest are

Table 3 Soma sizes (μm^2) of Purkinje cells, granule cells, and cerebellar nuclei neurons across species analyzed (± SD)

Order	Common name/species	Purkinje cell size	Granule cell size	Cerebellar nuclei neuron size
Accipitriformes	Collared sparrowhawk (*Accipiter cirrocephalus)*	300.710 ± 61.251	8.797 ± 1.256	334.739 ± 71.562
	Wedge-tailed eagle (*Aquila audax*)	456.756 ± 83.102	14.002 ± 2.896	479.626 ± 153.855
	White-bellied sea eagle (*Haliaeetus leucogaster)*	469.149 ± 112.661	11.225 ± 1.448	462.654 ± 141.603
Anseriformes	American wigeon (*Anas americana*)	459.791 ± 95.990	9.172 ± 1.434	405.114 ± 119.114
	Northern shoveler (*Anas clypeata*)	317.128 ± 71.180	10.069 ± 1.160	442.122 ± 106.362
	Mallard (*Anas platyrhynchos*)	476.699 ± 190.757	9.630 ± 1.254	348.200 ± 92.530
	Gadwall (*Anas strepera*)	247.916 ± 55.068	8.819 ± 1.534	336.350 ± 89.451
	Lesser scaup (*Aythya affinis*)	433.919 ± 106.203	11.824 ± 1.737	437.387 ± 155.998
	Bufflehead (*Bucephala albeola)*	343.081 ± 60.692	11.195 ± 1.136	392.749 ± 100.220
	Common goldeneye (*Bucephala clangula*)	511.195 ± 184.240	13.167 ± 2.318	395.496 ± 135.575
	Red-breasted merganser (*Mergus serrator*)	222.020 ± 43.691	9.056 ± 1.086	299.579 ± 88.618
Caprimulgiformes	Spotted nightjar (*Eurostopodus argus*)	274.709 ± 67.539	9.621 ± 1.241	271.130 ± 67.376
	Tawny frogmouth (*Podargus strigoides*)	511.705 ± 122.552	15.668 ± 2.285	437.580 ± 132.350
Casuariiformes	Emu (*Dromaius novaehollandiae*)	578.392 ± 110.782	20.144 ± 3.951	372.085 ± 95.745
Charadriiformes	Silver gull (*Larus novaehollandiae*)	400.590 ± 63.807	12.356 ± 2.210	329.251 ± 98.496
	Short-billed dowitcher (*Limnodromus griseus*)	304.695 ± 66.178	10.727 ± 1.252	345.054 ± 90.268
Columbiformes	Rock dove (*Columba livia*)	328.607 ± 70.135	14.038 ± 1.999	369.342 ± 114.043
	Peaceful dove (*Geopelia placida*)	331.634 ± 63.452	11.986 ± 1.885	354.633 ± 130.276
Coraciiformes	Laughing kookaburra (*Dacelo novaeguineae*)	347.044 ± 79.126	11.157 ± 1.527	434.509 ± 128.607
Falconiformes	Brown falcon (*Falco berigora*)	377.064 ± 97.670	10.932 ± 1.358	292.18 ± 63.169
Galliformes	Ruffed grouse (*Bonasa umbellus*)	417.338 ± 24.792	11.861 ± 1.337	408.100 ± 115.922
	Japanese quail (*Coturnix japonica*)	366.541 ± 25.575	13.602 ± 0.135	323.366 ± 73.456
	Spruce grouse (*Dendragapus canadensis*)	412.334 ± 66.047	13.459 ± 0.039	392.945 ± 89.769
	Turkey (*Meleagris gallopavo*)	501.821 ± 11.098	10.989 ± 0.078	412.496 ± 113.538
	Indian peafowl (*Pavo cristatus*)	529.581 ± 43.140	12.699 ± 1.754	501.634 ± 159.881
	Grey partridge (*Perdix perdix*)	403.532 ± 60.218	14.817 ± 0.849	401.63 ± 119.885
	Ring-necked pheasant (*Phasianus colchicus*)	481.987 ± 13.865	11.930 ± 0.736	372.831 ± 91.257
Gruiformes	American coot (*Fulica americana*)	397.465 ± 84.706	10.315 ± 1.325	371.351 ± 84.818
	Dusky moorhen (*Gallinula tenebrosa*)	322.775 ± 71.775	10.386 ± 1.363	385.486 ± 101.154
Otidiformes	Australian bustard (*Ardeotis australis*)	393.842 ± 106.024	10.666 ± 1.435	369.809 ± 98.759

Table 3 (continued)

Order	Common name/species	Purkinje cell size	Granule cell size	Cerebellar nuclei neuron size
Passeriformes	Brown thornbill (*Acanthiza pusilla*)	189.003 ± 34.175	6.306 ± 0.967	226.162 ± 49.399
	Little raven (*Corvus mellori*)	484.401 ± 115.573	9.369 ± 1.220	459.757 ± 130.644
	Australian magpie (*Gymnorhina tibicen*)	345.135 ± 66.720	9.555 ± 1.366	413.521 ± 112.178
	Superb lyrebird (*Menura novaehollandiae*)	280.407 ± 59.367	8.708 ± 1.000	357.912 ± 82.596
	Field sparrow (*Spizella pusilla*)	191.211 ± 44.279	9.904 ± 1.788	302.391 ± 79.363
Pelecaniformes	Cattle egret (*Bubulcus ibis*)	543.942 ± 130.684	10.780 ± 1.534	421.988 ± 129.709
	Australian pelican (*Pelecanus conspicillatus*)	492.731 ± 111.300	16.094 ± 2.686	457.406 ± 154.674
Piciformes	Scaly-throated honeyguide (*Indicator variegatus*)	292.638 ± 62.710	11.430 ± 1.963	310.044 ± 96.800
	Yellow-bellied sapsucker (*Sphyrapicus varius*)	166.29 ± 39.679	11.771 ± 1.916	252.462 ± 67.996
Procellariiformes	Short-tailed shearwater (*Puffinus tenuirostris*)	344.706 ± 107.151	10.537 ± 1.279	305.454 ± 80.332
	Black-browed albatross (*Thalassarche melanophris*)	343.577 ± 76.180	12.244 ± 1.518	362.104 ± 99.151
Psittaciformes	Australian king parrot (*Alisterus scapularis*)	404.644 ± 79.071	9.461 ± 1.071	359.630 ± 144.957
	Sulphur-crested cockatoo (*Cacatua galerita*)	423.260 ± 86.903	10.784 ± 1.412	488.317 ± 187.910
	Galah (*Cacatua roseicapilla*)	346.342 ± 67.906	9.531 ± 1.037	317.196 ± 69.466
	Purple-crowned lorikeet (*Glossopsitta porphyrocephala*)	315.535 ± 69.678	10.368 ± 1.121	451.154 ± 145.499
	Budgerigar (*Melopsittacus undulatus*)	317.18 ± 66.208	10.160 ± 1.309	383.317 ± 110.859
	Cockatiel (*Nymphicus hollandicus*)	384.595 ± 69.721	9.586 ± 1.287	403.847 ± 123.281
	Crimson rosella (*Platycercus elegans*)	349.493 ± 71.025	8.993 ± 1.317	327.510 ± 102.433
	Red-rumped parrot (*Psephotus haematonotus*)	307.785 ± 45.189	9.497 ± 1.434	337.123 ± 83.237
	Rainbow lorikeet (*Trichoglossus haematodus*)	377.526 ± 96.850	9.909 ± 1.065	294.431 ± 62.871
Sphenisciformes	Little penguin (*Eudyptula minor*)	512.358 ± 133.930	13.308 ± 1.924	383.633 ± 97.203
Strigiformes	Northern saw-whet owl (*Aegolius acadicus*)	305.544 ± 76.990	10.730 ± 1.191	319.019 ± 88.886
	Australian boobook (*Ninox boobook*)	269.488 ± 45.881	8.200 ± 1.258	235.656 ± 60.165
	Barn owl (*Tyto alba*)	385.962 ± 98.792	12.076 ± 1.682	356.918 ± 78.560

provided in Table 1. The distance between the grid points (grid size), and the sampling interval, varied according to overall cerebellum size (Table S1). The coefficients of error for all volumes ranged from 0.002 to 0.014.

Surface area of the Purkinje cell layer

The surface area of the Purkinje cell layer was calculated by measuring the total length of the Purkinje cell layer through the sagittal axis of the cerebellum, and multiplying it by the thickness of the Sects. (40 µm) and sampling interval (Table 1). The sampling interval was the same one used for the volumetric measurements (see Table S1).

Cerebellar foliation index (CFI)

We used the same approach as in Iwaniuk et al. (2006, 2009) to calculate the degree of foliation (i.e., folding) in the cerebellum (Table 1). First, we measured (a) the total length of the Purkinje cell layer of the midsagittal section and then (b) the length of the "envelope" enclosing the Purkinje cell layer (see Fig. 2a). The ratio (a/b) between these two measurements serves as a metric to calculate the degree of foliation, referred to as the cerebellar foliation index (CFI), and is comparable to gyrification indices calculated in mammals (Hofman 1985; Pillay and Manger 2007; Zilles et al. 1989). Thus, a higher number reflects a greater degree of foliation.

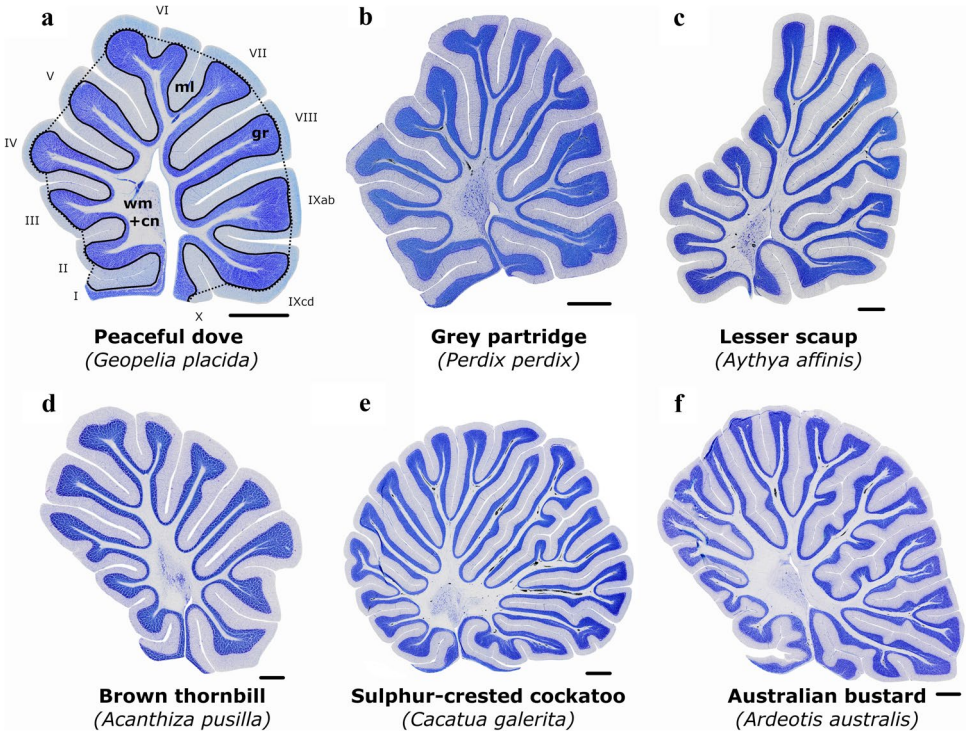

Fig. 2 Midsagittal sections of Nissl-stained cerebella of: **a** peaceful dove (*Geopelia placida*), **b** grey partridge (*Perdix perdix*), **c** lesser scaup (*Aythya affinis*), **d** brown thornbill (*Acanthiza pusilla*), **e** sulphur-crested cockatoo (*Cacatua galerita*), and **f** Australian bustard (*Ardeotis australis*). Note the difference in cerebellar size and shape across avian species. For example, while the sulphur-crested cockatoo has a CFI of 5.56, the peaceful dove has a CFI of 2.97. For the peaceful dove (A), cerebellar folia are represented as roman numerals, from I (anterior) to X (posterior), as suggested by Larsell (1967). The black continuous line follows the Purkinje cell layer. The ratio between the length of the Purkinje cell layer (continuous black line) and the envelope length of this same layer (dotted black line) is referred to as the cerebellar foliation index (CFI). *ml* molecular layer, *gr* granule cell layer, and "*wm*+*cn*" white matter layer and cerebellar nuclei. Scalebars: A–C = 1 mm, D = 0.5 mm, E–F = 2 mm

Cell counts

We estimated the number of three types of cerebellar neurons: Purkinje cells, granule cells, and cerebellar nuclei neurons (Table 2; Fig. S1). Purkinje cells are found exclusively within the Purkinje cell layer and are readily identifiable from other cerebellar cell types based on size, shape, and location. We only counted Purkinje cells with intact continuous cell membranes, typical "teardrop" shape, and clearly visible nuclei. The numbers of Purkinje cells were estimated using the optical fractionator method implemented in Stereo Investigator software (Microbrightfield Inc., VT, USA), with a 20 × objective (n.a. = 0.5) on a Zeiss Axio Imager 2 microscope. Frame size remained constant across all species, but grid size varied according to cerebellum size (Table S1). The coefficients of error (CE) of the Purkinje cell counts, defined as the standard error of the mean of repeated estimates divided by the mean (Microbrightfield Inc., VT; USA), were all equal to or below 0.05, indicating that our measurements were precise (Gundersen et al. 1999).

Granule cells are densely packed within the granule cell layer and it is possible to distinguish them from other neuron types within this layer by cellular morphology and spatial distribution (Fig. S1). Granule cells, however, cannot be necessarily discerned from non-neuronal cells (e.g., glia) in Nissl-stained tissue; thus, our granule cell counts likely represent an overestimation of granule cell numbers (Cunha et al. 2020). The fact that specimens in our lab collection were fixed, prepared and mounted previously, at different times, prevented us from using NeuN as a neuron-specific marker in the cerebellum (Mullen et al. 1992). Still, given that specimens were processed consistently by the same method, neuronal counts likely yield comparable numbers across species within our study.

We counted granule cells with continuous, round shaped, and intact cell membranes and darkly stained nuclei (Table 2), which distinguishes them from Lugaro, Golgi, and unipolar brush cells. Lugaro cells are either globular or spindle-like in shape, are mostly clustered just below the Purkinje cell layer (Craciun et al. 2019; Fox 1959). Golgi cells have an irregular shape, are much larger than granule cells and typically have pale cytoplasmic staining (Andersen et al. 1992; Dieudonné 1998). Last, unipolar brush cells have circular-ovoid somata and are intermediate in size between

granule cells and Golgi cells (Mugnaini and Floris 1994). Therefore, based on our morphological selection criteria, and given the low density of these other neuronal types, the potential inclusion of some is unlikely to affect our estimates of the total number of granule cells. The optical fractionator method was also used to quantify the numbers of granule cells under the same microscope with a 100 × objective (n.a. = 1.4). Frame size remained constant across species, but grid size varied (Table S1). Because granule cells are relatively small (< 20 µm^2) and densely packed (Fig. S1), they could be damaged or sectioned at the top and bottom surfaces of the tissue. Thus, guard zones of 4–7 µm were used to protect against lost caps (Gardella et al. 2003). All granule cell counts had CEs that were equal to or below 0.07.

Cerebellar nuclei neurons are distributed in two paired nuclei within the white matter layer (Arends and Zeigler 1991). Here, we counted all of them as a single population (Table 2) because it was not possible to define clear anatomical borders between the cerebellar nuclei in sagittal sections (see also above). We only counted cerebellar nuclei neurons with intact cell membranes. The shape and size of the soma of cerebellar nuclei neurons was highly variable, ranging from globular to fusiform-like shape (Fig. S1). As with other cells, we used the optical fractionator probe with the same microscope, and a 40 × objective (n.a. = 0.95), to estimate the numbers of cerebellar nuclei neurons. Frame size remained constant across species, but grid size varied (Table S1). To compensate and protect against lost caps, we used guard zones from 4 to 7 µm (Gardella et al. 2003). All cerebellar nuclei neuron counts had CEs that were equal to or below 0.07.

Cell sizes

We measured soma sizes of Purkinje cells, granule cells, and cerebellar nuclei neurons. All cell sizes were measured using the nucleator probe (4 rays), implemented in Stereo Investigator (Microbrightfield Inc., VT, USA). The nucleator probe estimates the average cross-sectional area of randomly selected neurons. For the current study, at least 100 size measurements were made of each neuronal type for each specimen (Table 3). The measurements for each cell size followed a typical normal distribution (see Fig. 3). For all neuron types, cell membranes were intact, and morphologies followed the descriptions provided above.

Variation across orders

Due to common ancestry, closely related species are expected to have more traits in common (Garamszegi 2014). Therefore, to examine allometric relationships among all measurements, we performed phylogenetic generalized least squares (PGLS) of log-transformed data. The aim of PGLS is to test hypotheses about correlated evolution, assuming that the residuals from a linear model have a phylogenetic covariance. All statistical analyses were performed in R 4.0.3 (R Core Team 2020), using the pgls function in *caper* (Orme et al. 2013) and *nlme* (Pinheiro et al. 2006) with maximum likelihood estimations of Pagel's λ (Pagel 1999). We extracted 1000 fully resolved trees from birdtree.org (Jetz et al. 2012), with Ericson et al. (2006) backbone phylogeny, and built a maximum clade credibility tree (consensus tree; Fig. 1) using *phangorn* (Schliep 2011). For all PGLS analyses, we used log-transformed data and the consensus phylogenetic tree. We ran phylogenetic analyses of covariance (pANCOVA) to test for significant differences across clades. We specifically tested for allometric differences across avian orders that have at least five species represented in our sample: *Anseriformes* (waterfowl), *Galliformes* (chicken-like birds), *Passeriformes* (songbirds), and *Psittaciformes* (parrots). Species from all other clades were lumped together as "other birds". Because *Galliformes* and *Anseriformes* form a monophyletic group ("Galloanserae") and *Passeriformes* and *Psittaciformes* form another monophyletic group ("Psittacopasserae") (Hackett et al. 2008; Jarvis et al. 2014; Prum et al. 2015), we also ran separate statistical analyses for both of these clades against "other birds". The percentage differences reported in the results (see below) are based on the differences between the intercepts and/or slopes for a given clade (e.g., *Galliformes*) and other birds.

Model selection and hypothesis testing

To test whether surface area of the Purkinje cell layer or cerebellar volume better explains the variation of the Purkinje cell number, we compared allometric models using Akaike information criterion (AIC) values to identify the most parsimonious model (Burnham and Anderson 2002, 2004).

Results

Allometric relationships of the cerebellum volume

The molecular, granule cell, and white matter plus cerebellar nuclei (wm + cn) layers increased with the rest of the cerebellum with slopes that approximated isometry (Table S2; Fig. 4). The scaling of the molecular layer did not differ significantly across clades (Fig. 4a), but galliforms had relatively smaller granule cell layer (− 38%; Fig. 4b; pANCOVA, $p = 0.01$; no differences in slopes) and wm + cn volumes compared with other birds (− 11%; Fig. 4c; pANCOVA, $p < 0.01$; no differences in slopes). In contrast, parrots had significantly larger wm + cn volumes than other birds (+ 10%; Fig. 4c; pANCOVA, $p = 0.04$; no differences

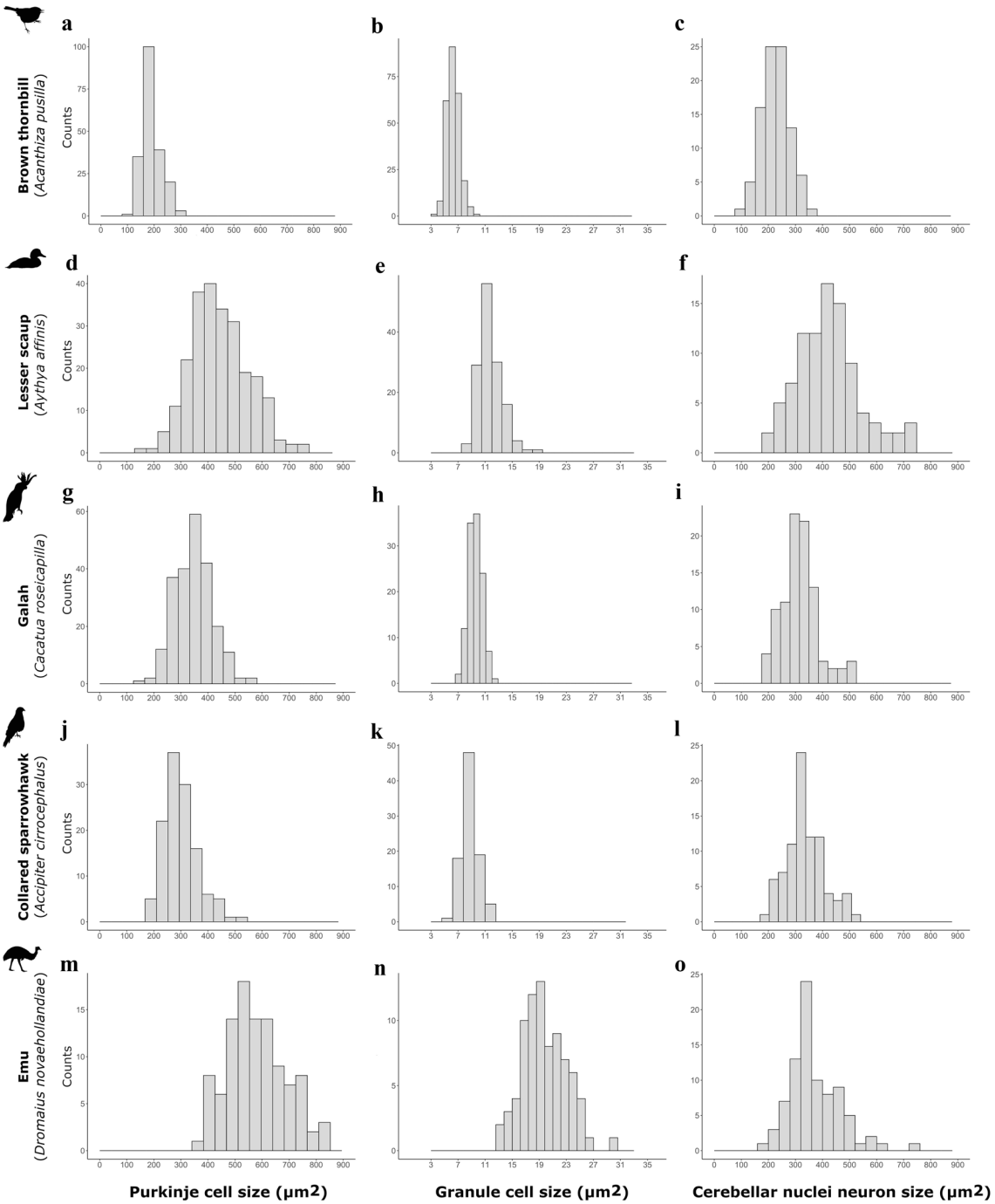

Fig. 3 Distribution of cell soma sizes (μm^2) of Purkinje cells (**a**, **d**, **g**, **j**, **m**), granule cells (**b**, **e**, **h**, **k**, **n**), and cerebellar nuclei neurons (**c**, **f**, **i**, **l**, **o**) within the following specimens: brown thornbill (*Acanthiza pusilla,* **a**–**c**), lesser scaup (*Aythya affinis,* **d**–**f**), galah (*Cacatua roseicapilla*, **g**–**i**), collared sparrowhawk (*Accipiter cirrocephalus*, **j**–**l**) and emu (*Dromaius novaehollandiae*, **m**–**o**). The depicted bars represent the summed-up counts of cells within the following ranges: 25–50 µm for Purkinje cells and cerebellar nuclei neurons, and 0.75–1.50 µm for granule cells. The distribution of cell soma sizes followed a normal distribution curve. Although the distribution of the granule cell sizes in the emu appears to be slightly different than a normal curve, most of the measurements were still restricted to a narrow range of sizes (e.g., 16–22 µm)

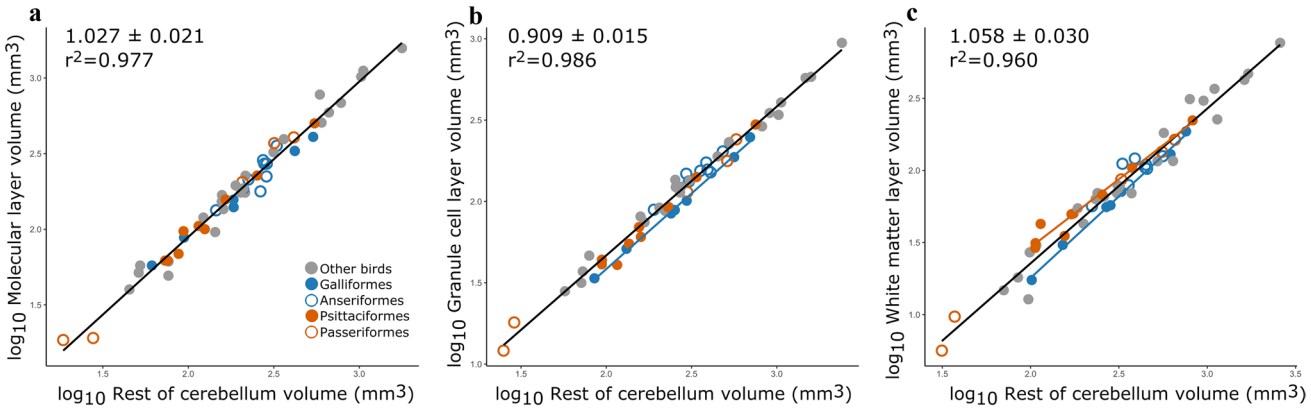

Fig. 4 Scatterplots of the log-transformed volumes (mm^3) of: **a** molecular layer (mm^3) against rest of cerebellum and **b** granule cell layer against rest of the cerebellum, **c** white matter layer plus cerebellar nuclei neurons against rest of the cerebellum. Clades with significant differences from other birds are indicated in the graph. See allometric equations and statistical data in Table S2. The rest of the cerebellum refers to as total cerebellum size minus the size of the cerebellar layer in the y-axis

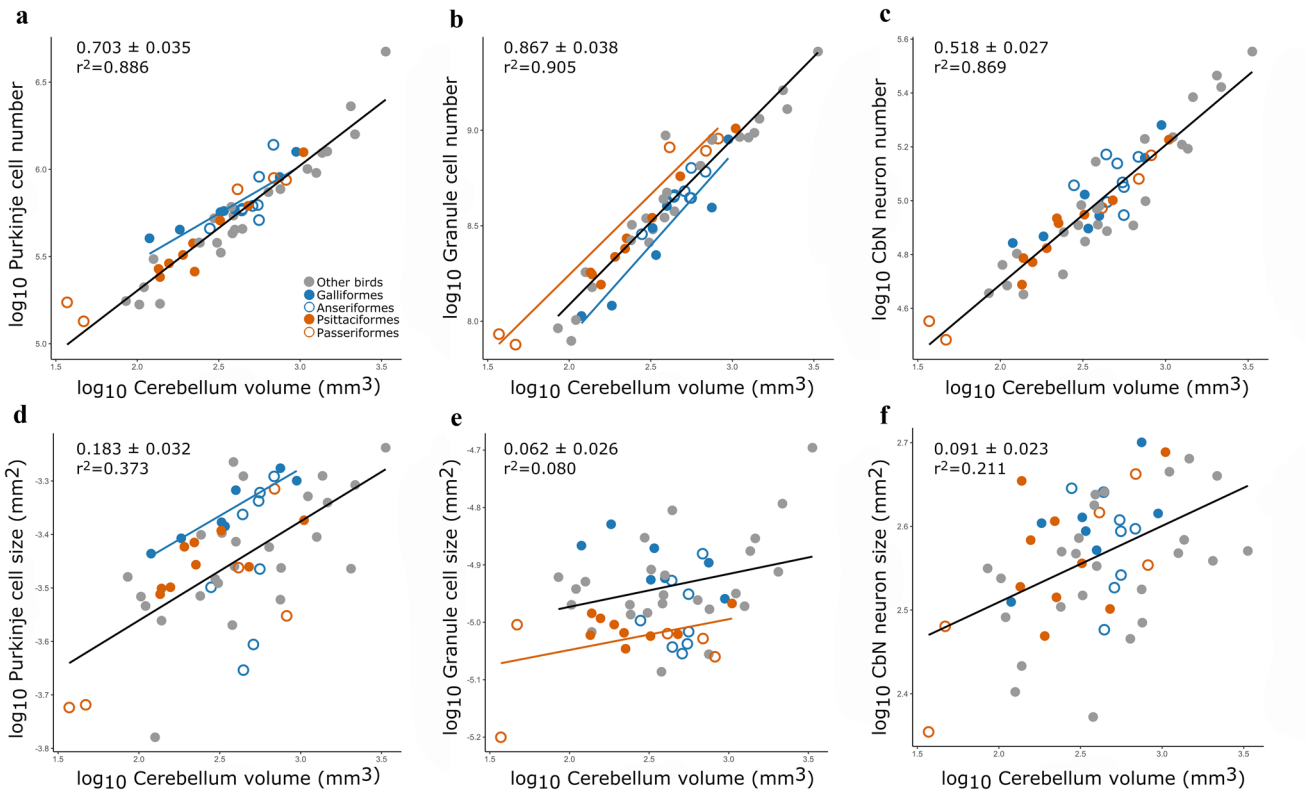

Fig. 5 Scatterplots of the log-transformed of: **a** Purkinje cell number, **b** granule cell number, **c** cerebellar nuclei neuron number, **d** Purkinje cell size (mm^2), **e** granule cell size (mm^2), and **f** cerebellar nuclei neuron size (mm^2) against the log-transformed volume (mm^3) of the cerebellum. Clades with significant differences from other birds are indicated in the graph. See allometric equations and statistical data in Table S2. *CbN* cerebellar nuclei

in slopes). Note that despite these significant differences, there was quite a bit of overlap across clades (Fig. 4).

The number of Purkinje cells increased with cerebellar volume with a slope less than 1 (slope = 0.703 ± 0.035 (standard error); PGLS, $p < 0.01$; Fig. 5a; Table S2). The only clade that differed significantly from this allometric relationship was Galliformes, which had relatively more Purkinje cells (+ 2.5%; Fig. 5a; pANCOVA, $p = 0.01$; no differences in slopes). Waterfowl did not differ significantly from other groups and, therefore, the difference between

Galliformes and other clades also drove a significant, but marginal, difference in relative Purkinje cell numbers between Galloanserae and other birds (+1.6%, Fig. 5a; pANCOVA, $p=0.04$; no differences in slopes). Granule cells increased in number with cerebellum volume with a steeper slope than that of Purkinje cells (0.867 ± 0.038, PGLS, $p<0.01$; Fig. 5b; Table S2). Across clades, galliforms had significantly fewer granule cells relative to cerebellar volume (− 2.1%; Fig. 5b; pANCOVA, $p<0.01$; no differences in slopes) and songbirds have significantly more granule cells (+2.4%, Fig. 5b; pANCOVA, $p<0.01$). Last, the number of cerebellar nuclei neurons increases significantly with the cerebellum volume, but with the shallowest slope of the three neuron types (0.518 ± 0.027; Fig. 5c; PGLS, $p<0.01$; Table S2) and no significant differences were detected across clades.

As shown in Fig. 3, cell sizes varied greatly within species (coefficients of variation = 20–30%). Average cell sizes scaled at different slopes relative to total cerebellar volume (Table S2) and the slopes were much shallower than that for cell numbers (Fig. 5). Across clades, Galliformes have significantly larger Purkinje cells relative to cerebellar volume than other birds (+4.7%, Fig. 5d; pANCOVA, $p<0.01$; no differences in slopes). At the other end of the spectrum, songbirds have significantly smaller granule cells relative to cerebellum size than other birds, which also drove a significant difference between Psittacopasserae and other birds (− 9%; Fig. 5e; pANCOVA, $p=0.01$; no slope differences). No significant differences were detected across orders or clades for the size of the cerebellar nuclei neurons relative to the volume of the cerebellum (Fig. 5f; Table S2).

Allometric relationships among neuronal populations

Among the three neuronal populations, allometric relationships varied in strength and slope. The number of granule cells increased with positive allometry relative to the number of Purkinje cells (1.125 ± 0.064; Fig. 6a; PGLS, $p<0.01$; Table S2). Across clades, galliforms had significantly fewer granule cells relative to the number of Purkinje cells compared to other birds (− 11%, Fig. 6a; pANCOVA, $p<0.01$)

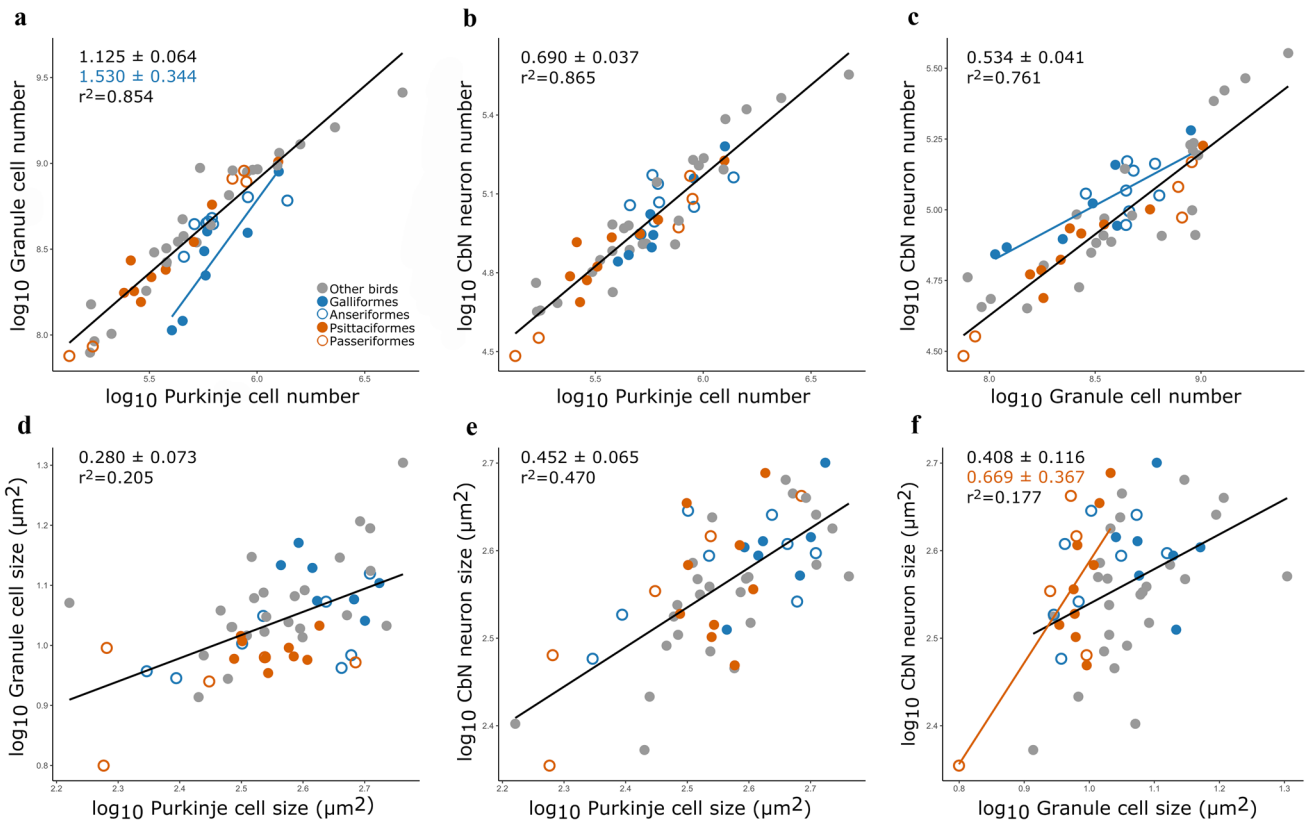

Fig. 6 Scatterplots of the log-transformed of: **a** granule cell number against Purkinje cell number, **b** cerebellar nuclei neuron number against Purkinje cell number, **c** cerebellar nuclei neuron number against granule cell number, **d** granule cell size (μm^2) against Purkinje cell size (μm^2), **e** cerebellar nuclei neuron size (μm^2) against Purkinje cell size, and **f** cerebellar nuclei neuron size against granule cell size. Clades with significant differences from other birds are indicated in the graph. See allometric equations and statistical data in Table S2. *CbN* cerebellar nuclei

and drove a significant difference between Galloanserae and other birds (− 7%, Fig. 6a; pANCOVA, $p = 0.01$). Galliformes also had a steeper slope for the granule cell-Purkinje cell relationship compared to other birds (+36%, Fig. 6a; pANCOVA, $p = 0.03$). The number of cerebellar nuclei neurons increased with the number of Purkinje cells with a much shallower slope than the number of granule cells (0.690 ± 0.037; Fig. 6b; PGLS, $p < 0.01$; Table S2), and no significant differences were detected among clades. The number of cerebellar nuclei neurons increased with the number of granule cells with the shallowest slope (0.534 ± 0.041; Fig. 6c; PGLS, $p < 0.01$; Table S2). As shown in Fig. 6c, Galliformes had significantly more cerebellar nuclei neurons relative to granule cells than other birds (+41%; Fig. 6c; pANCOVA, $p = 0.01$) and this also drove significant differences between Galloanserae and other birds (+28%; Fig. 6c; pANCOVA, $p < 0.01$; no slope differences).

Allometric relationships among the sizes of the three neuronal populations also varied in strength and slope. The size of granule cells increased with the size of Purkinje cells with the shallowest slope (0.280 ± 0.073; Fig. 6d; PGLS, $p < 0.01$; Table S2). The size of cerebellar nuclei neurons increased with the size of Purkinje cells with a much steeper slope (0.452 ± 0.065; Fig. 6e; PGLS, $p < 0.01$; Table S2). Lastly, the size of cerebellar nuclei neurons increased significantly with the size of granule cells with a slope similar to that of the Purkinje cells (0.408 ± 0.116; Fig. 6f; PGLS, $p < 0.01$; Table S2). The only difference detected among clades is that the Psittacopasserae had a higher slope (+64%) for the relationship between cerebellar nuclei and granule cell sizes (Fig. 6f; pANCOVA, $p = 0.04$). This difference remains significant (pANCOVA, $p < 0.05$) when excluding an outlier (the brown thornbill (*Acanthiza pusilla*); Fig. 6f).

When plotting the numbers of each neuronal population against neuron size, no significant differences were detected across clades (Fig. 7). The number of Purkinje cells increased with the size of Purkinje cells with a slope close to isometry (1.105 ± 0.246; Fig. 7a; PGLS, $p < 0.01$; Table S2). Similarly, the number of cerebellar nuclei neurons increased with the size of cerebellar nuclei neurons with a slope close to 1 (0.983 ± 0.311; Fig. 7b; PGLS, $p < 0.01$; Table S2). However, for both of these relationships, the coefficients of correlation were no higher than 0.265 (see Table S2). For granule cells, the relationship between neuron number and neuron size was not significant (PGLS, $p > 0.05$; Fig. 7c; Table S2).

Allometry of cerebellar foliation and surface area

As demonstrated in previous studies (Cunha et al. 2020; Iwaniuk et al. 2005), the avian cerebellum increased in volume relative to the rest of the brain with isometry (slope = 0.934 ± 0.046, PGLS, $p < 0.01$; Table S2; Fig. 8a), although parrots and songbirds (Psittacopasserae) had relatively smaller cerebella (− 18%; Fig. 8a; pANCOVA, $p = 0.01$; no differences in slopes). However, Iwaniuk et al. (2006) noted that the cerebellum is more foliated in these groups, as measured by the CFI, and suggested that the surface area of the cerebellum and the number of Purkinje cells would be higher in relation to cerebellar volume. When we plotted the surface area of the Purkinje cell layer against the rest of brain size (0.752 ± 0.044; Fig. 8b; PGLS, $p < 0.01$), and number of Purkinje cells against the rest of brain size (0.656 ± 0.048; Fig. 8c; PGLS, $p < 0.01$; Table S2), parrots and songbirds did not differ from other clades (Fig. 8b, c). These data support the inferences of Iwaniuk et al. (2006): despite having a relatively smaller cerebellum, parrots and songbirds do not have a smaller surface area or number of Purkinje cells relative to the rest of the brain.

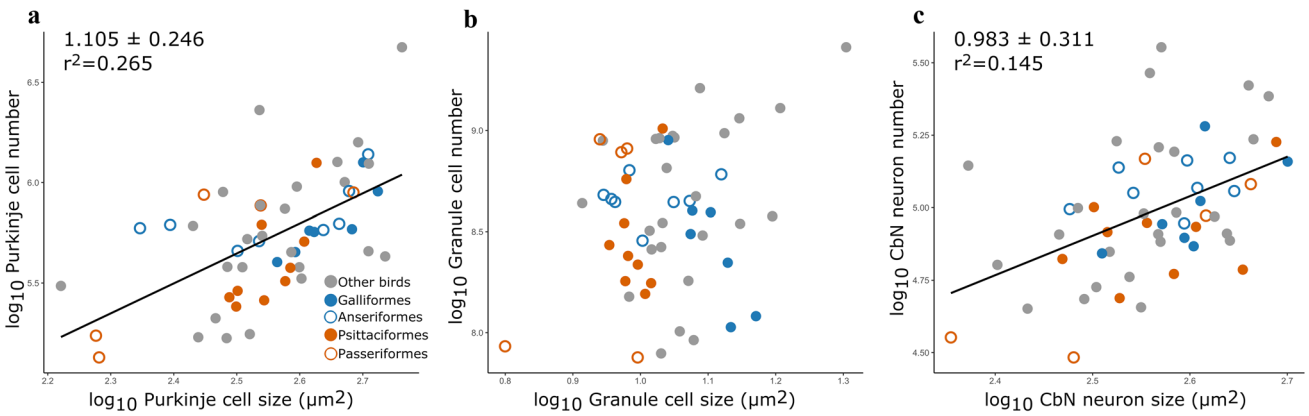

Fig. 7 Scatterplots of the log-transformed of: **a** Purkinje cell number against Purkinje cell size (μm^2), **b** granule cell number against granule cell size (μm^2), and **c** cerebellar nuclei neuron number against cerebellar nuclei neuron size (μm^2). See allometric equations and statistical data in Table S2

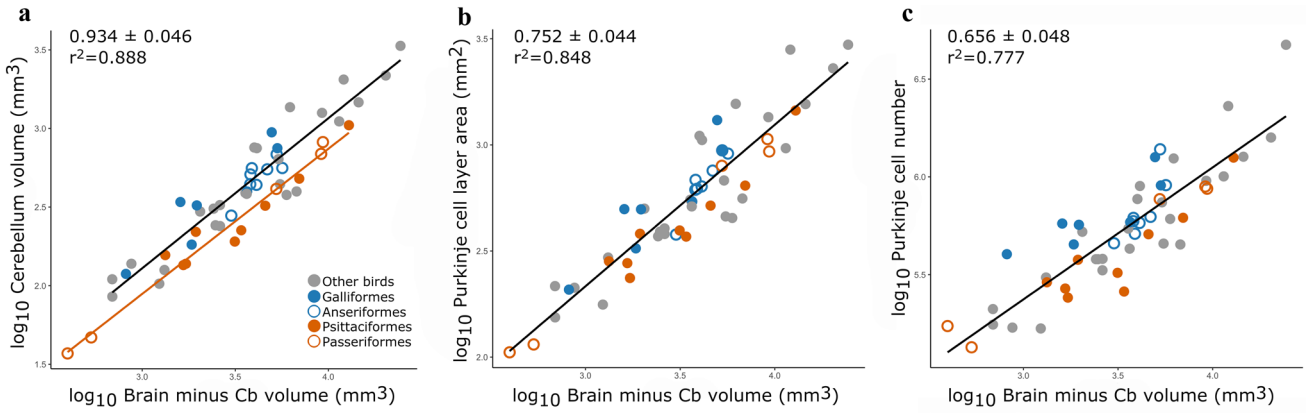

Fig. 8 Scatterplots of the log-transformed of: **a** cerebellum volume (mm^3) against rest of the brain volume (mm^3), **b** surface area of Purkinje cell layer (mm^2) against rest of the brain volume, and **c** Purkinje cell number against rest of the brain volume. Clades with significant differences from other birds are indicated in the graph. See allometric equations and statistical data in Table S2

However, the same data plotted relative to cerebellar volume yielded contradictory evidence. First, as shown above in Fig. 5a, the number of Purkinje cells relative to cerebellar volume is not higher for parrots and songbirds. Second, when the surface area of the Purkinje cell layer is plotted against cerebellar volume (Fig. 9a, Table S2) most of the parrots and songbirds lie above the regression line, but there were no significant differences across clades detected. Nonetheless, when we ran multiple allometric models to determine whether cerebellar volume or surface area of the Purkinje cell layer best explained the number of Purkinje cells (Figs. 5a, 9b; Table S3), Purkinje cell layer surface area was the best predictor of the number of Purkinje cells (dAIC > 2; Table S3).

We then plotted CFI against cerebellar volume (Fig. 9c), Purkinje cell layer surface area (Fig. 9d) and number of Purkinje cells (Fig. 9e). In all three plots, parrots and songbirds are shifted to the left, indicating significantly higher CFI values relative to all three scaling variables. This grade shift indicates that the CFI is a poor proxy, specifically an overestimate, for both measures of cerebellar surface area and Purkinje cell numbers in parrots and songbirds.

Discussion

As found previously within galliform birds (Cunha et al. 2020), the expansion of the cerebellum across bird species is due to coordinated changes in volume across cerebellar layers such that no one layer increases in size more than another. Despite conservation of the proportional volumes of the layers, the numbers and sizes of different neuronal populations have different allometric relationships with cerebellar volume, and several differences among clades were detected (see Table 4).

Despite these overall patterns, a few caveats should be considered in interpreting our data and analyses. First, some avian/clades are represented by more species than others. We, therefore, cannot negate the possibility that there are other differences among clades that we were unable to detect due to small sample sizes. Second, we sampled only one individual of most species. The morphology of the cerebellum can vary significantly within species (El-Andari et al. 2020; Escalona et al. 1991; Inouye and Oda 1980; Puzdrowski and Leonard 1992), but variation in brain or brain region size is usually higher across species than within species (Herculano-Houzel et al. 2014, 2015a, b) and the intraspecific coefficients of variation for the measurements on galliform species are typically lower than 15% (see Cunha et al. 2020; El-Andari et al. 2020). Although the specific slopes and intercepts of the various allometric relationships described herein might shift with the addition of more individuals per species and/or more species overall, the general patterns are unlikely to change. We also stress that it remains unclear to what extent fixation affects cell density or cell size. Given that our specimens were processed following the same procedure, this potential artifact is unlikely to affect our main findings, but could still affect direct comparisons between our data and future studies using different histological procedures. Last, our granule cell counts likely include non-neuronal cells (e.g., glia) and, therefore, represent an overestimation of total granule cell numbers. Because of that, our data cannot be compared directly with that of isotropic fractionation studies (Olkowicz et al. 2016) and the allometric equations that include granule cell numbers should be interpreted with caution. For example, when comparing the number of cerebellar neurons in the six species (*Cacatua galerita*, *Columba livia*, *Dromaius novaehollandiae*,

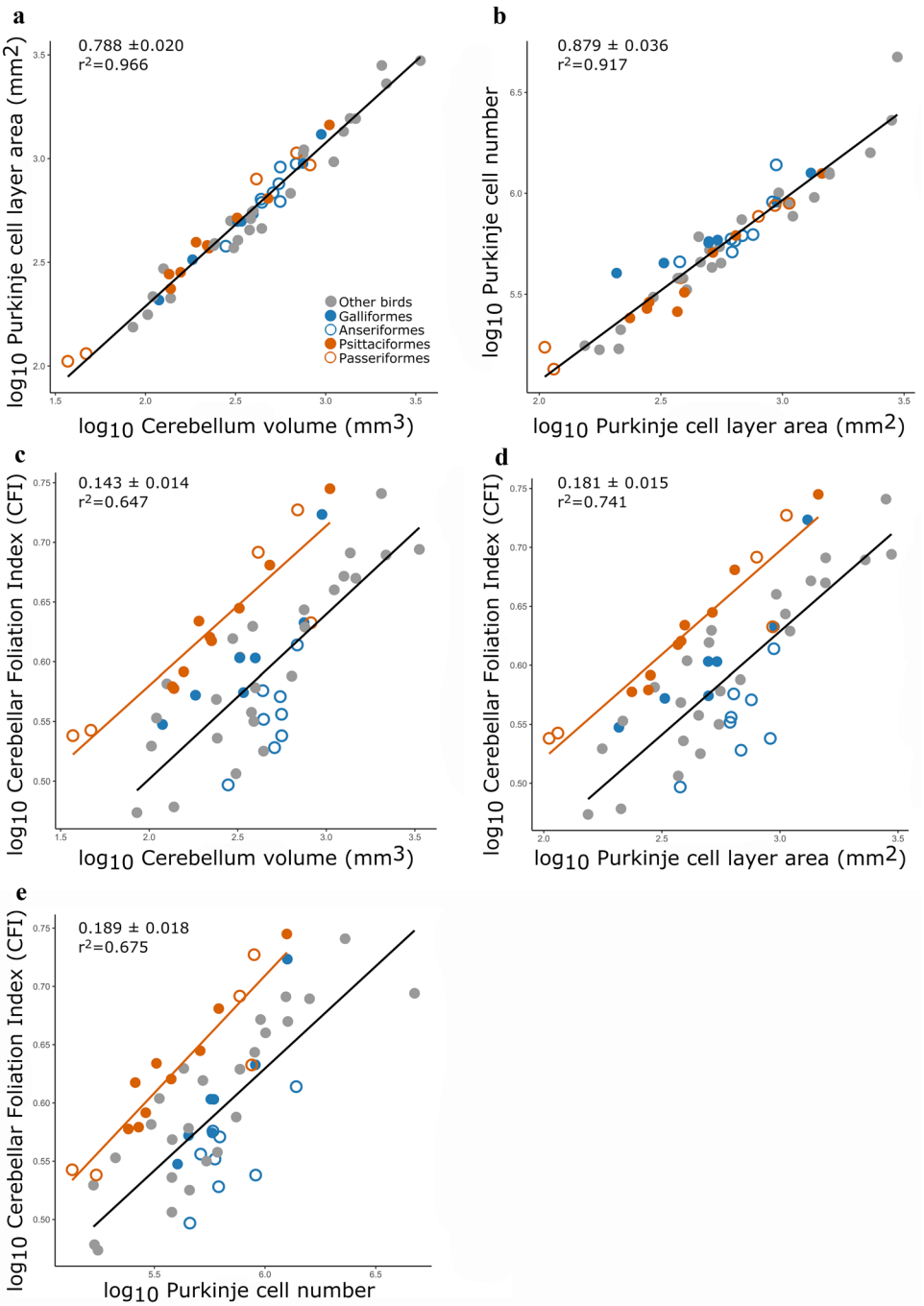

Fig. 9 Scatterplots of the log-transformed of: **a** surface area of the Purkinje cell layer (mm^2) against cerebellum volume (mm^3), **b** Purkinje cell number against surface area of the Purkinje cell layer, **c** cerebellar foliation index (CFI) against cerebellum volume, **d** cerebellar foliation index against surface area of the Purkinje cell layer, and **e** cerebellar foliation index against Purkinje cell number. Clades with significant differences from other birds are indicated in the graph. See allometric equations and statistical data in Table S2

Melopsittacus undulatus, *Nymphicus hollandicus*, *Tyto alba*) examined in this study and Olkowicz et al (2016), our study reports on average two times more cerebellar neurons than Olkowicz et al (2016). We also note that the brain sizes for the six species mentioned above were on average 1.2 times larger in our study than in Olkowicz et al. (2016). Nevertheless, our data are the most comprehensive to date for a comparative study and provides some novel insights into cerebellar evolution.

Allometric scaling within the cerebellum

The cerebellum has an anatomical organization that is highly conserved across most species, including the connectivity patterns across neuronal populations (Voogd and Glickstein 1998; Yopak et al. 2017). This pattern of connectivity is not only preserved across vertebrate species, but also across different functional units within the cerebellum itself (Apps et al. 2018; Voogd and Glickstein 1998; Yopak et al. 2017). It is, therefore, unsurprising that all three cerebellar layers

Table 4 Summary of the clade differences for the measurements examined relative to brain volume (vol.) or cerebellum volume

Measurements/order	Anseriformes	Galliformes	Passeriformes	Psittaciformes
Cerebellum vol	–	–	↓	↓
Molecular layer vol	–	–	–	–
Granule layer vol	–	↓	–	–
WM + Cb vol	–	↓	–	↑
#Purkinje cells	–	↑	–	–
Purkinje cell size	–	↑	–	–
#Granule cells	–	↓	↑	–
Granule cell size	–	–	↓	–
#CbN neurons	–	–	–	–
#CbN neuron size	–	–	–	–
Purkinje surface area	–	–	–	–
CFI	–	–	↑	↑

Down arrow indicates relative reduction, up arrow indicates relative increase, and hyphen indicates no difference between a given clade and other birds

change in volume in a concerted fashion, with little deviation across clades. As shown in Fig. 4, there is little scatter around the allometric lines and the correlation coefficients (r^2 s in Table S2) are all above 0.95, indicating that interspecific variation in the absolute and relative size of the whole cerebellum largely arises from coordinated, volumetric increases across cell layers.

In contrast to the strong, nearly isometric relationships among layer volumes, larger cerebella have lower neuronal densities, a pattern that is typical of most brain regions and clades, regardless of whether the data are acquired through stereology (Cunha et al. 2020; Haug 1987; Lange 1975; Sherwood et al. 2020) or isotropic fractionation (Olkowicz et al. 2016; Herculano-Houzel et al. 2014, 2015a). There are, however, differences in the slope and strength of the neuron number-cerebellum volume relationship (i.e., r^2) among the three neuronal populations (see Table S2). Relative to cerebellar volume, the number of granule cells increases faster than the number of Purkinje cells, which increases faster than the number of cerebellar nuclei neurons (Fig. 5; Cunha et al. 2020). Thus, different types of neurons vary in their scaling relationship with brain region size and, by extension, a constant scaling pattern (or neuronal scaling "rule" sensu Herculano-Houzel et al. 2014) does not apply uniformly to cerebellar neurons and is unlikely to apply to other brain regions. In much the same way that volumetric measurements have moved away from large, multifunctional brain regions to functionally specific regions and/or circuits (Corfield et al. 2015; Gutiérrez-Ibáñez et al. 2011, 2013; Moore and DeVoogd 2017; Smaers and Vanier 2019; Vanier et al. 2019), the quantification of neuron numbers should extend to different neuronal populations and the role they have in neural circuits, to better understand how the brain evolves.

In addition to neuron numbers, we also estimated neuron sizes by measuring soma areas. Relative to cerebellum volume, neuron sizes increase at a significantly slower rate (see Fig. 5), and with much lower correlation coefficients (r^2 s = 0.08–0.37) than neuron numbers (r^2 s = 0.87–0.90). Thus, our results suggest that neuron size, relative to cerebellum volume, is more likely to vary across species than relative neuron numbers. The fact that neuron sizes are highly variable within a single neuronal population (see Fig. 3) might also explain why neuron size is much more variable than neuron number across species. As shown with neuron numbers (see above), each neuron type also scaled at a different rate with cerebellar volume. Neuron size is not discussed as frequently as neuron numbers in comparative studies, but it is an important contributor to brain region volume and information processing capacity (Chang et al. 2020; de Sousa and Proulx 2014; Smith et al. 1997). Although soma size is only one metric of neuron size, it is often associated with the physiological properties of a neuron (Chang et al. 2020; Cooper and Stanford 2000; Meitzen and Thompson 2008). For example, variation in soma size of Purkinje cells can reflect firing type and input resistance (Chang et al. 2020), and larger cells tend to have larger or more organelles, such as the endoplasmic reticulum and mitochondria (Reber and Goehring 2015), which would potentially enable higher energetic capacity (Marshall 2015; Reber and Goehring 2015). Relatively larger (or smaller) neurons within a clade, therefore, might reflect physiological differences that are relevant to behaviour. However, what those differences might be is entirely speculative as little is known about differences in motor control and coordination across bird species. Regardless of the functional correlates and implications of neuron size, our data indicate neuron size cannot be inferred accurately from neuron numbers due to differences in the allometric scaling of neuron size and numbers across neuronal populations (see Figs. 6, 7). Moreover, as shown in Fig. 3, neuron size is highly variable within a single neuronal population, and for that reason estimations of neuron size from neuronal density (see Herculano-Houzel et al. 2014) are likely inaccurate.

One of the few exceptions to the general patterns observed across species is the order Galliformes. Galliforms have smaller granule cell and white matter layer-cerebellar nuclei ("wm + cn") layers relative to the size of the rest of the cerebellum compared to other birds (Fig. 4), even though they do not have relatively small cerebella (Fig. 8a). The molecular layer in galliforms is not proportionally expanded (Fig. 4a), indicating that the relative decrease in the other layers is due to a change in Purkinje cells. Accurately measuring the volume of the Purkinje cell layer is not possible due to frequent gaps between Purkinje cells (see "Methods"), but

galliforms do have more and larger Purkinje cells relative to the size of the cerebellum (Fig. 5), which would result in a larger Purkinje cell layer. Why galliforms differ from other clades in these scaling relationships is unclear, but some insights might be gleaned by examining the cerebella of behaviorally and ecologically similar clades, such as tinamous (Tinamiformes), bustards (Otidiformes), and/or buttonquail (Turnicidae).

Cerebellar volume, surface area of the Purkinje cell layer, and foliation

Parrots and songbirds have relatively smaller cerebellar volumes (Fig. 8a; Iwaniuk et al. 2006), but a greater degree of foliation, as measured by a higher midsagittal CFI (Fig. 9c–e). In previous studies, this measure was considered a proxy for surface area and Purkinje cell number (Hall et al. 2013; Iwaniuk et al. 2009). That is, parrots and songbirds may have a smaller cerebellum by volume, but an increase in the foliation provides a larger surface area and thus a greater processing capacity for the cerebellum. In the present study, we actually measured the surface area of the cerebellum and the number of Purkinje cells. On the one hand, we found that relative to the rest of the brain, the surface area of the cerebellum and the number of Purkinje cells is not reduced in parrots and songbirds despite smaller cerebellar volumes (see Fig. 8). This is further supported by the cerebellar surface area being a better predictor of Purkinje cell number than cerebellar volume (see Figs. 5a, 9b). Thus, the increase in cerebellar foliation in parrots and songbirds maintains the processing capacity of a smaller cerebellum, a functionality that might be required for their expanded telencephala (Boire and Baron 1994; Iwaniuk et al. 2005). On the other hand, parrots and songbirds did not significantly increase surface area or Purkinje cell number relative to cerebellar volume (see Figs. 5a, 9a). We must, therefore, conclude that any effects of foliation are weak and that the midsagittal CFI is not a good proxy for surface area or number of Purkinje cells. This is very apparent in Figs. 9d–e, where the CFI grossly overestimates the surface area and number of Purkinje cells in parrots and songbirds. Intuitively, this should not come as a surprise. In birds the cerebellum is folded only in the anterior–posterior dimension, which is not the case in sharks (Yopak et al. 2007, 2017), the cerebellar hemispheres in mammals (Smaers et al. 2018; Voogd and Glickstein 1998) or the cerebral cortex in mammals (Pillay and Manger 2007; Zilles et al. 1989). Thus, in birds the CFI is maximal in the midsagittal section, and progressively approaches 1.0 as one moves laterally to the flocculus and lateral unfoliated cortex. The result is that the midsagittal CFI overestimates total foliation, and by extension also overestimates surface area and Purkinje cell number.

Conclusions

Our results show that cerebellar layers increase in size proportionally and the numbers of cerebellar neurons explain more variation in cerebellar volume than the sizes of cerebellar neurons. Thus, despite all the species differences in cerebellar size and shape (Cunha et al. 2020; Macrì et al. 2019; Smaers et al. 2018), the conserved pattern of cerebellar connectivity across species is reflected in proportional increases in size of the cerebellar layers. Within this general framework, we also found that different neuronal populations have different allometric scaling rules relative to the size of the cerebellum, thus indicating that measuring total neuron numbers within larger brain regions (Herculano-Houzel et al. 2014; Olkowicz et al. 2016) might not provide a complete picture of the relationship between neuron numbers and brain region sizes. Given that patterns of cerebellar connectivity are relatively uniform across vertebrate species (Yopak et al. 2017), we expect to find similar changes across the volumes of cerebellar layers in other vertebrate clades, but also varying allometric scaling patterns across neuronal populations in the cerebellum. Testing the extent to which these patterns are conserved in the cerebellum across all vertebrates would provide insights into the putative mechanisms responsible for clade differences in relative cerebellum size and morphology.

Supplementary Information The online version contains supplementary material available at https://doi.org/10.1007/s00429-021-02352-2.

Acknowledgements We wish to thank Maurice Needham and Ben Brinkman for assistance with microscopy.

Author contributions All authors had full access to all the data in the study and take responsibility for the integrity of the data and the accuracy of the data analysis. FC, DW, and ANI: study concept and design. FC, and KR: acquisition of the data. FC, CGI, DR, and ANI: analysis and interpretation of the data. FC, CGI, DR, and ANI: drafting of the manuscript. FC, KR, CGI, DR, and ANI: critical revision of the manuscript for important intellectual content, administrative, technical, and material support.

Funding Funding to support this study was provided by scholarships to FC from the University of Lethbridge, NSERC Discovery grants to DRW and ANI and the Canada Foundation for Innovation and Canada Research Chairs Program to ANI.

Data availability All data generated and analysed in this study are included in the article.

Code availability Not applicable.

Declarations

Conflict of interest The authors declare that the research was conducted in the absence of any commercial or financial relationships that could be construed as a potential conflict of interest.

Ethical approval Not applicable.

Consent to participate Not applicable.

Consent for publication Not applicable.

References

Andersen BB, Korbo L, Pakkenberg B (1992) A quantitative study of the human cerebellum with unbiased stereological techniques. J Comparative Neurol 326(4):549–560

Apps R, Hawkes R (2009) Cerebellar cortical organization: a one-map hypothesis. Nat Rev Neurosci 10(9):670–681

Apps R, Hawkes R, Aoki S, Bengtsson F, Brown AM, Chen G, Ebner TJ, Isope P, Jörntell H, Lackey EP (2018) Cerebellar modules and their role as operational cerebellar processing units. Cerebellum 17(5):654–682

Arends J, Zeigler HP (1991) Organization of the cerebellum in the pigeon (Columba livia): II. Projections of the cerebellar nuclei. J Comparative Neurol 306(2):245–272

Boire D, Baron G (1994) Allometric comparison of brain and main brain subdivisions in birds. J Brain Res 35(1):49–66

Burnham KP, Anderson DR (2002) Model selection and multimodel inference. A practical information-theoretic approach, 2nd edn. Springer, New York. https://doi.org/10.1007/b97636

Burnham KP, Anderson DR (2004) Multimodel inference: understanding AIC and BIC in model selection. Sociol Methods Res 33(2):261–304

Chang W, Pedroni A, Hohendorf V, Giacomello S, Hibi M, Köster RW, Ampatzis K (2020) Functionally distinct Purkinje cell types show temporal precision in encoding locomotion. Proc Natl Acad Sci 117(29):17330–17337

Cooper A, Stanford I (2000) Electrophysiological and morphological characteristics of three subtypes of rat globus pallidus neurone in vitro. J Physiol 527(2):291–304

Corfield JR, Birkhead TR, Spottiswoode CN, Iwaniuk AN, Boogert NJ, Gutiérrez-Ibáñez C, Overington SE, Wylie DR, Lefebvre L (2013) Brain size and morphology of the brood-parasitic and cerophagous honeyguides (Aves: Piciformes). Brain Behav Evol 81(3):170–186

Corfield JR, Price K, Iwaniuk AN, Gutiérrez-Ibáñez C, Birkhead T, Wylie DR (2015) Diversity in olfactory bulb size in birds reflects allometry, ecology, and phylogeny. Front Neuroanat 9:102

Craciun I, Gutierrez-Ibanez C, Chan AS, Luksch H, Wylie DR (2019) Secretagogin immunoreactivity reveals lugaro cells in the pigeon cerebellum. Cerebellum 18(3):544–555

Cunha F, Racicot K, Nahirney J, Heuston C, Wylie DR, Iwaniuk AN (2020) Allometric scaling rules of the cerebellum in Galliform birds. Brain Behav Evol 95(2):78–92

de Sousa AA, Proulx MJ (2014) What can volumes reveal about human brain evolution? A framework for bridging behavioral, histometric, and volumetric perspectives. Front Neuroanat 8:51

Dieudonné S (1998) Submillisecond kinetics and low efficacy of parallel fibre-Golgi cell synaptic currents in the rat cerebellum. J Physiol 510(3):845–866

El-Andari R, Cunha F, Tschirren B, Iwaniuk AN (2020) Selection for divergent reproductive investment affects neuron size and foliation in the cerebellum. Brain Behav Evol 95(2):69–77

Ericson PG, Anderson CL, Britton T, Elzanowski A, Johansson US, Källersjö M, Ohlson JI, Parsons TJ, Zuccon D, Mayr G (2006) Diversification of neoaves: integration of molecular sequence data and fossils. Biol Let 2(4):543–547

Escalona P, McDonald W, Doraiswamy P, Boyko O, Husain M, Figiel G, Laskowitz D, Ellinwood E, Krishnan K (1991) In vivo stereological assessment of human cerebellar volume: effects of gender and age. Am J Neuroradiol 12(5):927–929

Fox CA (1959) The intermediate cells of Lugaro in the cerebellar cortex of the monkey. J Comparative Neurol 112(1):39–53

Garamszegi LZ (2014) Modern phylogenetic comparative methods and their application in evolutionary biology: concepts and practice. Springer, Heidelberg

Gardella D, Hatton WJ, Rind HB, Rosen GD, von Bartheld CS (2003) Differential tissue shrinkage and compression in the z-axis: implications for optical disector counting in vibratome-, plastic-and cryosections. J Neurosci Methods 124(1):45–59

Gundersen H, Jensen E, Kiêu K, Nielsen J (1999) The efficiency of systematic sampling in stereology—reconsidered. J Microsc 193(3):199–211

Gutiérrez-Ibáñez C, Iwaniuk AN, Wylie DR (2011) Relative size of auditory pathways in symmetrically and asymmetrically eared owls. Brain Behav Evol 78(4):286–301

Gutiérrez-Ibáñez C, Iwaniuk AN, Lisney TJ, Wylie DR (2013) Comparative study of visual pathways in owls (Aves: Strigiformes). Brain Behav Evol 81(1):27–39

Hackett SJ, Kimball RT, Reddy S, Bowie RC, Braun EL, Braun MJ, Chojnowski JL, Cox WA, Han K-L, Harshman J (2008) A phylogenomic study of birds reveals their evolutionary history. Science 320(5884):1763–1768

Hall ZJ, Street SE, Healy SD (2013) The evolution of cerebellum structure correlates with nest complexity. Biol Let 9(6):20130687

Haug H (1987) Brain sizes, surfaces, and neuronal sizes of the cortex cerebri: a stereological investigation of man and his variability and a comparison with some mammals (primates, whales, marsupials, insectivores, and one elephant). Am J Anat 180(2):126–142

Herculano-Houzel S, Lent R (2005) Isotropic fractionator: a simple, rapid method for the quantification of total cell and neuron numbers in the brain. J Neurosci 25(10):2518–2521

Herculano-Houzel S, Manger PR, Kaas JH (2014) Brain scaling in mammalian evolution as a consequence of concerted and mosaic changes in numbers of neurons and average neuronal cell size. Front Neuroanat 8:77

Herculano-Houzel S, Catania K, Manger PR, Kaas JH (2015a) Mammalian brains are made of these: a dataset of the numbers and densities of neuronal and nonneuronal cells in the brain of glires, primates, scandentia, eulipotyphlans, afrotherians and artiodactyls, and their relationship with body mass. Brain Behav Evol 86(3–4):145–163

Herculano-Houzel S, Messeder DJ, Fonseca-Azevedo K, Pantoja NA (2015b) When larger brains do not have more neurons: increased numbers of cells are compensated by decreased average cell size across mouse individuals. Front Neuroanat 9:64

Herculano-Houzel S, von Bartheld CS, Miller DJ, Kaas JH (2015c) How to count cells: the advantages and disadvantages of the isotropic fractionator compared with stereology. Cell Tissue Res 360(1):29–42

Hofman MA (1985) Size and shape of the cerebral cortex in mammals (part 1 of 2). Brain Behav Evol 27(1):28–40

Inouye M, Oda SI (1980) Strain-specific variations in the folial pattern of the mouse cerebellum. J Comparative Neurol 190(2):357–362

Iwaniuk AN, Dean KM, Nelson JE (2005) Interspecific allometry of the brain and brain regions in parrots (Psittaciformes): comparisons with other birds and primates. Brain Behav Evol 65(1):40–59

Iwaniuk AN, Lefebvre L, Wylie DR (2009) The comparative approach and brain–behaviour relationships: a tool for understanding tool use. Can J Exp Psychol/revue Canadienne De Psychologie Expérimentale 63(2):150

Iwaniuk AN, Hurd PL, Wylie DR (2006) Comparative morphology of the avian cerebellum: I. Degree of foliation. Brain Behav Evol 68(1):45–62

Iwaniuk AN, Hurd PL, Wylie DR (2007) Comparative morphology of the avian cerebellum: II. Size of folia. Brain Behav Evol 69(3):196–219

Jardim-Messeder D, Lambert K, Noctor S, Pestana FM, de Castro Leal ME, Bertelsen MF, Alagaili AN, Mohammad OB, Manger PR, Herculano-Houzel S (2017) Dogs have the most neurons, though not the largest brain: trade-off between body mass and number of neurons in the cerebral cortex of large carnivoran species. Front Neuroanat 11:118

Jarvis ED, Mirarab S, Aberer AJ, Li B, Houde P, Li C, Ho SY, Faircloth BC, Nabholz B, Howard JT (2014) Whole-genome analyses resolve early branches in the tree of life of modern birds. Science 346(6215):1320–1331

Jetz W, Thomas GH, Joy JB, Hartmann K, Mooers AO (2012) The global diversity of birds in space and time. Nature 491(7424):444–448

Lange W (1975) Cell number and cell density in the cerebellar cortex of man and some other mammals. Cell Tissue Res 157(1):115–124

Lange W (1982) Regional differences in the cytoarchitecture of the cerebellar cortex. In: Palay SL, Chan-Palay V (eds) The cerebellum. New vistas. Exp Brain Res Suppl 6. Springer, Berlin, Heidelberg, pp 93–107

Larsell O (1967) The cerebellum: from myxinoids through birds. University of Minnesota Press, Minneapolis

MacLeod CE, Zilles K, Schleicher A, Rilling JK, Gibson KR (2003) Expansion of the neocerebellum in Hominoidea. J Hum Evol 44(4):401–429

Macrì S, Savriama Y, Khan I, Di-Poï N (2019) Comparative analysis of squamate brains unveils multi-level variation in cerebellar architecture associated with locomotor specialization. Nat Commun 10(1):1–16

Marshall WF (2015) How cells measure length on subcellular scales. Trends Cell Biol 25(12):760–768

Meitzen J, Thompson CK (2008) Seasonal-like growth and regression of the avian song control system: neural and behavioral plasticity in adult male Gambel's white-crowned sparrows. Gen Comp Endocrinol 157(3):259–265

Moore JM, DeVoogd TJ (2017) Concerted and mosaic evolution of functional modules in songbird brains. Proc R Soc B 284(1854):20170469

Mugnaini E, Floris A (1994) The unipolar brush cell: a neglected neuron of the mammalian cerebellar cortex. J Comparative Neurol 339(2):174–180

Mullen RJ, Buck CR, Smith AM (1992) NeuN, a neuronal specific nuclear protein in vertebrates. Development 116(1):201–211

Ngwenya A, Nahirney J, Brinkman B, Williams L, Iwaniuk AN (2017) Comparison of estimates of neuronal number obtained using the isotropic fractionator method and unbiased stereology in day old chicks (*Gallus domesticus*). J Neurosci Methods 287:39–46

Olkowicz S, Kocourek M, Lučan RK, Porteš M, Fitch WT, Herculano-Houzel S, Němec P (2016) Birds have primate-like numbers of neurons in the forebrain. Proc Natl Acad Sci 113(26):7255–7260

Orme D, Freckleton R, Thomas G, Petzoldt T, Fritz S, Isaac N, Pearse W (2013) The caper package: comparative analysis of phylogenetics and evolution in R. R Package Vers 5(2):1–36

Pagel M (1999) The maximum likelihood approach to reconstructing ancestral character states of discrete characters on phylogenies. Syst Biol 48(3):612–622

Pillay P, Manger PR (2007) Order-specific quantitative patterns of cortical gyrification. Eur J Neurosci 25(9):2705–2712

Pinheiro J, Bates D, DebRoy S, Sarkar D, Team RC (2006) nlme: linear and nonlinear mixed effects models. R Package Vers 3(4):109

Prum RO, Berv JS, Dornburg A, Field DJ, Townsend JP, Lemmon EM, Lemmon AR (2015) A comprehensive phylogeny of birds (Aves) using targeted next-generation DNA sequencing. Nature 526(7574):569–573

Puzdrowski RL, Leonard RB (1992) Variations in cerebellar morphology of the Atlantic stingray. Dasyatis Sabina Neurosci Lett 135(2):196–200

R Core Team (2020) R: a language and environment for statistical computing. R Foundation for Statistical Computing, Vienna, Austria

Reber S, Goehring NW (2015) Intracellular scaling mechanisms. Cold Spring Harb Perspect Biol 7(12):a019067

Schliep KP (2011) Phangorn: phylogenetic analysis in R. Bioinformatics 27(4):592–593

Sherwood CC, Miller SB, Karl M, Stimpson CD, Phillips KA, Jacobs B, Hof PR, Raghanti MA, Smaers JB (2020) Invariant synapse density and neuronal connectivity scaling in primate neocortical evolution. Cereb Cortex 30(10):5604–5615

Smaers JB, Turner AH, Gómez-Robles A, Sherwood CC (2018) A cerebellar substrate for cognition evolved multiple times independently in mammals. Elife 7:e35696

Smaers JB, Vanier DR (2019) Brain size expansion in primates and humans is explained by a selective modular expansion of the cortico-cerebellar system. Cortex 118:292–305

Smith GT, Brenowitz EA, Beecher MD, Wingfield JC (1997) Seasonal changes in testosterone, neural attributes of song control nuclei, and song structure in wild songbirds. J Neurosci 17(15):6001–6010

Stevens C (1969) Structure of cat frontal olfactory cortex. J Neurophysiol 32(2):184–192

Sultan F, Glickstein M (2007) The cerebellum: comparative and animal studies. Cerebellum 6(3):168–176

Teeter CM, Stevens CF (2011) A general principle of neural arbor branch density. Curr Biol 21(24):2105–2108

Vanier DR, Sherwood CC, Smaers JB (2019) Distinct patterns of hippocampal and neocortical evolution in primates. Brain Behav Evol 93(4):171–181

Voogd J, Glickstein M (1998) The anatomy of the cerebellum. Trends Cogn Sci 2(9):307–313

Yopak KE, Lisney TJ, Collin SP, Montgomery JC (2007) Variation in brain organization and cerebellar foliation in chondrichthyans: sharks and holocephalans. Brain Behav Evol 69(4):280–300

Yopak KE, Pakan J, Wylie D (2017) The cerebellum of nonmammalian vertebrates. In: Kaas JH (ed) Evolution of nervous systems, 2nd edn. Academic Press, Oxford, pp 373–386

Zilles K, Armstrong E, Moser KH, Schleicher A, Stephan H (1989) Gyrification in the cerebral cortex of primates. Brain Behav Evol 34(3):143–150